

# Inferring Covariance Structure from Multiple Data Sources via Subspace Factor Analysis

Noirrit Kiran Chandra<sup>†</sup>, David B. Dunson<sup>‡</sup>, Jason Xu<sup>‡,\*</sup>

<sup>†</sup>Department of Mathematical Sciences,  
The University of Texas at Dallas, Richardson, TX  
Email: noirrit.chandra@utdallas.edu

<sup>‡</sup>Department of Statistical Science, Duke University, Durham, NC

\*Department of Biostatistics and Bioinformatics, Duke University, Durham, NC

## Abstract

Factor analysis provides a canonical framework for imposing lower-dimensional structure such as sparse covariance in high-dimensional data. High-dimensional data on the same set of variables are often collected under different conditions, for instance in reproducing studies across research groups. In such cases, it is natural to seek to learn the shared versus condition-specific structure. Existing hierarchical extensions of factor analysis have been proposed, but face practical issues including identifiability problems. To address these shortcomings, we propose a class of SUbspace Factor Analysis (SUFA) models, which characterize variation across groups at the level of a lower-dimensional subspace. We prove that the proposed class of SUFA models lead to identifiability of the shared versus group-specific components of the covariance, and study their posterior contraction properties. Taking a Bayesian approach, these contributions are developed alongside efficient posterior computation algorithms. Our sampler fully integrates out latent variables, is easily parallelizable and has complexity that does not depend on sample size. We illustrate the methods through application to integration of multiple gene expression datasets relevant to immunology.

*Keywords:* Data-augmented Markov chain Monte Carlo, Data Integration, Gradient-Based Sampling, Latent Variable Models, Multi-Study Factor Analysis.

## 1 Introduction

With increasing calls for reproducibility and transparency in science, it has become standard to make datasets widely available to the scientific community. This motivates interest in aggregating different but related datasets together. A prominent

example arises in gene network analyses where it is of interest to merge datasets from studies that consider a common set of genes. Combining datasets increases sample size in studying covariance structure among the genes. To conduct principled inference, it is important to account for differences across studies, and not simply pool the data. This article focuses on developing statistical methods for inferring common versus study-specific covariance structures, with a particular motivation to multi-study applications in the high-dimensional setting. These methods immediately apply to data from a single study featuring hierarchical, multi-group structure as well.

Consider the analysis of gene expression levels in immune cells. Integrating data from multiple studies serves to (1) increase statistical precision in making inferences on covariance structure between genes; (2) yield results that are more robust to study-to-study variability and hence more generalizable; and (3) obtain insight into shared versus study-specific contributors to the covariance. We focus on datasets from the Immunological Genome Project ([Heng \*et al.\*, 2008](#)), comprising microarray assays as well as bulk RNA sequencing data as shown in Figure S.3 in the supplementary materials. Substantial similarity between the datasets can be observed albeit with significant amount of heterogeneity. Such heterogeneity is typical and arises due to differences between the subject populations, and variation in data collection technologies inducing platform-specific effects in the respective datasets.

Given our interest in the covariance structure of high-dimensional data, it is natural to consider Bayesian sparse factor analysis (FA) models, which achieve state-of-the-art performance in the single-study case ([Fan \*et al.\*, 2008](#); [Knowles and Ghahramani, 2011](#); [Trendafilov \*et al.\*, 2017](#)). Even when different studies collect the same variables for closely-related populations, applying factor analysis separately to each dataset can lead to very different inferred factor structures. There are recent ap-

proaches extending factor analysis to the multi-study setting—notably, [De Vito \*et al.\* \(2019, 2021\)](#) proposed a conceptually simple multi-study FA model. This appealing model includes shared and study-specific components via an additive expansion but is known to face identifiability issues, discussed further below. Alternatively, [Roy \*et al.\* \(2021\)](#) proposed a multiplicative ‘perturbed’ FA model that focuses on inferring the shared structure while making use of subject-specific perturbations to resolve identifiability issues in post-processing steps.

Motivated by surmounting the identifiability issues arising in multi-study factor analysis, we propose a novel shared *SUBspace Factor Analysis (SUFA)* model. In particular, SUFA assumes that there is a common lower-dimensional subspace shared across the multiple studies under consideration. The data from different studies all provide partial information about the shared subspace, providing a mechanism for borrowing of information. Moreover, this subspace is the key in yielding identifiability of the common versus study-specific components of the covariance. Related work by [Franks and Hoff \(2019\)](#) focuses on identifying the *best* shared subspace across groups. In contrast, we focus on learning the shared versus study-specific contributors to covariance structure. Our factor analysis approach allows one to infer latent factors jointly with the structure of their loadings, providing valuable interpretations in applications including gene expression studies ([Iacob \*et al.\*, 2016](#)).

We focus on identifiability up to the usual rotational ambiguity encountered in factor modeling. Then, following standard practice in the Bayesian factor modeling literature, we rotationally align the factors across MCMC iterations in a post-processing stage. By using a fast algorithm recently introduced by [Poworoznek \*et al.\* \(2021\)](#), we maintain sparsity in the post-processed samples of the loadings by leveraging a key sparsity-inducing property of the varimax rotation ([Kaiser, 1958](#); [Rohe](#)

and Zeng, 2020). Sparse loadings have considerable interpretability advantages; for example, a subset of genes that loads onto a particular factor is commonly interpreted as belonging to the same pathway.

To provide theoretical support in terms of covariance estimation, we derive favorable posterior contraction rates for subspace factor models in a high-dimensional setting. Our analysis shows that the shared covariance structure can be recovered with added precision for each additional study, even when the marginal distributions of data differ substantially across studies. Although the classical factor analysis literature relies heavily on choosing the number of latent factors correctly, we show that our covariance matrix estimation is robust to this choice.

Our model is developed alongside computational contributions to enable efficient posterior inference. Latent variable-based Gibbs sampling (Bhattacharya and Dunson, 2011; Sabnis *et al.*, 2016) or expectation-maximization (EM) algorithms (Ročková and George, 2016) are the most popular approaches for Bayesian factor models. However, the conditional updating can become a computational bottleneck for massive sample sizes, further exacerbated in multi-study settings. Dai *et al.* (2020) proposed a fast matrix-free approach for exploratory factor analysis but their approach does not apply in Bayesian contexts. We develop a scalable (large  $n$ ) Hamiltonian Monte Carlo (HMC, Neal, 2011) sampler that jointly updates parameters while marginalizing out latent factors. This leads to significant improvements in mixing relative to Gibbs sampling. The proposed sampler depends only on the study-specific sample covariance matrices, which can be computed and cached prior to running MCMC. The computational complexity is then essentially invariant of the sample size, and we design a distributed computing framework to parallelize each MCMC iteration.

The remainder of the article is organized as follows: Section 2 describes the SUFA

model, and 2.1 discusses and resolves the potential identifiability issues common to multi-study factor models. Section 2.2 discusses our choice of prior and other important specifications. Section 3 establishes posterior contraction rates in high-dimensional settings. These contributions are made practical in Section 4, where we propose a scalable HMC algorithm for posterior sampling. Section 5.1 compares SUFA with existing approaches via a suite of simulation studies, and the methods are applied in an integrative gene network analysis case study in Section 5.2. We close by discussing our contributions and future directions in Section 6.

## 2 Bayesian SUbspace Factor Analysis (SUFA)

In this article, we consider the setting where data consist of  $S$  studies each comprising  $d$ -variate observations  $\mathbf{Y}_{s,i} = (Y_{s,i,1}, \dots, Y_{s,i,d})^T$ ,  $i = 1, \dots, n_s$ ,  $s = 1, \dots, S$  measured on the same set of features with  $\mathbf{Y}_{s,i} \stackrel{\text{iid}}{\sim} N(\boldsymbol{\mu}_s, \boldsymbol{\Sigma}_s)$ . Without loss of generality, we assume  $\boldsymbol{\mu}_s = \mathbf{0}$  following standard practice to center the data. In our motivating application, we seek to jointly learn from two microarray datasets and a bulkRNASeq dataset: we have  $S = 3$  studies each analyzing  $d = 474$  genes. In studying the correlation structure between genes, we expect a common fundamental association between features across the studies, along with study-specific variations. Hence, we let  $\boldsymbol{\Sigma}_s = \boldsymbol{\Sigma} + \boldsymbol{\Gamma}_s$  where  $\boldsymbol{\Sigma}$  is a positive definite matrix quantifying the shared structure, and  $\boldsymbol{\Gamma}_s$  accounts for the respective study-specific dependencies.

Bayesian factor analysis often yields state-of-the-art performance in single-study high-dimensional covariance estimation (Bhattacharya and Dunson, 2011; Pati *et al.*, 2014; Ročková and George, 2016). Adopting a usual factor-analytic covariance factorization as the sum of a low rank and diagonal matrix to the shared  $\boldsymbol{\Sigma}$ , we let  $\boldsymbol{\Sigma} = \boldsymbol{\Lambda}\boldsymbol{\Lambda}^T + \boldsymbol{\Delta}$ , where  $\boldsymbol{\Lambda}$  is a  $d \times q$  factor loading matrix, with  $q \ll d$  the number

of latent factors, and  $\Delta = \text{diag}(\delta_1^2, \dots, \delta_d^2)$  is a diagonal matrix of residual variances.

Evidence in the literature suggests that expression-level dependent error variances tend to produce better results (Kepler *et al.*, 2002), so we do not assume  $\Delta = \sigma^2 \mathbf{I}_d$ .

To model the study-specific deviations, we let  $\Gamma_s = \Lambda \mathbf{A}_s \mathbf{A}_s^T \Lambda^T$ , where  $\mathbf{A}_s$  is a  $q \times q_s$  matrix. This leads to the following expression for the covariance specific to study  $s$ :  $\Sigma_s = \Lambda \Lambda^T + \Lambda \mathbf{A}_s \mathbf{A}_s^T \Lambda^T + \Delta$ . This can equivalently be written

$$\mathbf{Y}_{s,i} = \Lambda \boldsymbol{\eta}_{s,i} + \Lambda \mathbf{A}_s \boldsymbol{\zeta}_{s,i} + \boldsymbol{\epsilon}_{s,i}, \quad \boldsymbol{\eta}_{s,i} \stackrel{\text{iid}}{\sim} N_q(\mathbf{0}, \mathbf{I}_q), \quad \boldsymbol{\zeta}_{s,i} \stackrel{\text{iid}}{\sim} N_{q_s}(\mathbf{0}, \mathbf{I}_{q_s}), \quad \boldsymbol{\epsilon}_{s,i} \stackrel{\text{iid}}{\sim} N_d(\mathbf{0}, \Delta), \quad (1)$$

where  $\boldsymbol{\eta}_{s,i}$  is a  $q$  dimensional latent factor in the shared subspace,  $\boldsymbol{\zeta}_{s,i}$  are study-specific latent factors of dimension  $q_s$ , and  $\boldsymbol{\epsilon}_{s,i}$  are mean zero Gaussian error terms. Because  $\boldsymbol{\eta}_{s,i}$  are supported on the same subspace, our hierarchical model allows borrowing of information across studies in estimating  $\Sigma = \Lambda \Lambda^T + \Delta$ . This is formalized in Section 3. Model (1) implies the following marginal distributions

$$\mathbf{Y}_{s,i} \stackrel{\text{iid}}{\sim} N_d(\mathbf{0}, \Lambda \Lambda^T + \Lambda \mathbf{A}_s \mathbf{A}_s^T \Lambda^T + \Delta) \text{ for } s = 1, \dots, S. \quad (2)$$

Typically we take  $q_s < q$ , as integrative analyses of multiple studies are meaningful when the signals are mostly shared across studies. Imposing that  $q_s < q$  allows  $\Lambda$  to be the dominant term explaining the variation across the studies. The following sections make this intuition rigorous, and show how it ensures identifiability.

**Related work:** Under the same data organization, De Vito *et al.* (2019, 2021) define the multi-study factor analysis (MSFA) model:

$$\mathbf{Y}_{s,i} = \Lambda \boldsymbol{\eta}_{s,i} + \Phi_s \boldsymbol{\zeta}_{s,i} + \boldsymbol{\epsilon}_{s,i}, \quad \boldsymbol{\eta}_{s,i} \stackrel{\text{iid}}{\sim} N_q(\mathbf{0}, \mathbf{I}_q), \quad \boldsymbol{\zeta}_{s,i} \stackrel{\text{iid}}{\sim} N_{q_s}(\mathbf{0}, \mathbf{I}_{q_s}), \quad \boldsymbol{\epsilon}_{s,i} \stackrel{\text{iid}}{\sim} N_d(\mathbf{0}, \Delta_s), \quad (3)$$

where  $\Lambda$  is the  $d \times q$  shared factor loading matrix and  $\Phi_s$ 's are the  $d \times q_s$  study-specific loading matrices, with the remaining notation matching ours above. In contrast to (2), the implied marginal distribution is  $\mathbf{Y}_{s,i} \stackrel{\text{iid}}{\sim} N_d(\mathbf{0}, \Lambda \Lambda^T + \Phi_s \Phi_s^T + \Delta_s)$ . While

clearly related, this formulation assumes separate arbitrary  $d \times q_s$  matrices  $\Phi_s$  and residual error variances  $\Delta_s$  for each study. This may seem more flexible, but gives rise to a critical identifiability issue—the data can be fitted equally well if the shared  $\Lambda$  is completely ignored. This has adverse practical implications, especially in high-dimensional applications; Section 2.1 details how our method avoids these pitfalls.

Perturbed factor analysis (PFA, [Roy et al., 2021](#)) takes an altogether different approach with the same aim of learning shared covariance structure:

$$\mathbf{Q}_s \mathbf{Y}_{s,i} = \Lambda \boldsymbol{\eta}_{s,i} + \boldsymbol{\epsilon}_{s,i}, \quad \boldsymbol{\eta}_{s,i} \stackrel{\text{iid}}{\sim} N(\mathbf{0}, \mathbf{I}_q), \quad \boldsymbol{\epsilon}_{s,i} \stackrel{\text{iid}}{\sim} N(\mathbf{0}, \Delta), \quad (4)$$

where  $\Lambda$  is the  $d \times q$  common factor loading matrix,  $\mathbf{Q}_s$  is a  $d \times d$  perturbation matrix, and the remaining notation as above. Though it overcomes some of the pitfalls of the MSFA models, the study-specific effects cannot be recovered under PFA, and the introduction of  $\mathbf{Q}_s$  makes it difficult to scale beyond a few hundred dimensions.

## 2.1 Model Identifiability Guarantees

Factor analytic models such as SUFA are prone to two key identifiability issues:

**(I) Information Switching:** If there exists a  $q \times q$  non-null symmetric matrix  $\mathbf{C}$  such that  $\mathbf{I}_q - \mathbf{C} \succ \mathbf{0}$  and  $\mathbf{A}_s \mathbf{A}_s^T + \mathbf{C} = \tilde{\mathbf{A}}_s \tilde{\mathbf{A}}_s^T$  for some  $q \times q_s$  matrix  $\tilde{\mathbf{A}}_s$  for all  $s = 1, \dots, S$ , then multiple choices of  $\Lambda$  and  $\mathbf{A}_s$  yield the same marginal distribution in (2), leading to an identifiability issue between  $\Lambda$  and the  $\Lambda \mathbf{A}_s$ 's.

**(II) Rotational Ambiguity:** Let  $\tilde{\Lambda} = \Lambda \mathbf{H}$  and  $\tilde{\mathbf{A}}_s = \mathbf{H}^T \mathbf{A}_s \mathbf{H}_s$  where  $\mathbf{H}$  and  $\mathbf{H}_s$ 's are orthogonal matrices of order  $q \times q$  and  $q_s \times q_s$  respectively. Then substituting  $\Lambda$  and  $\mathbf{A}_s$ 's by  $\tilde{\Lambda}$  and  $\tilde{\mathbf{A}}_s$ 's respectively in (2) yields identical marginal distributions. This *information switching* is a crucial issue if  $\Sigma = \Lambda \Lambda^T + \Delta$  is to be interpreted as the shared covariance term, since  $\Sigma$  will not be identifiable. To establish some

intuition, we consider an example where  $d = 5$ ,  $S = 2$ ,  $q = 3$  with  $q_1 = q_2 = 2$ ,

$$\boldsymbol{\Lambda} = \begin{bmatrix} 7 & 5 & 6 \\ 6 & 6 & 7 \\ 6 & 9 & 4 \\ 5 & 5 & 6 \\ 4 & 6 & 6 \end{bmatrix}, \quad \mathbf{A}_1 = \begin{bmatrix} 3 & 0 \\ 0 & 2 \\ 0 & 0 \end{bmatrix} \quad \text{and} \quad \mathbf{A}_2 = \begin{bmatrix} 0 & 0 \\ 2 & 0 \\ 0 & 4 \end{bmatrix}. \quad (5)$$

Under the SUFA model, we can write  $\mathbf{Y}_{s,i} = [\boldsymbol{\Lambda} \quad \boldsymbol{\Lambda}\mathbf{A}_s] \begin{bmatrix} \boldsymbol{\eta}_{s,i} \\ \boldsymbol{\zeta}_{s,i} \end{bmatrix} + \boldsymbol{\epsilon}_{s,i}$ . This implies that for each of the two “studies”,  $\mathbf{Y}_{s,i}$  is given by

$$\mathbf{Y}_{1,i} = \underbrace{\begin{bmatrix} 7 & 5 & 6 & 21 & 10 \\ 6 & 6 & 7 & 18 & 12 \\ 6 & 9 & 4 & 18 & 18 \\ 5 & 5 & 6 & 15 & 10 \\ 4 & 6 & 6 & 12 & 12 \end{bmatrix}}_{\boldsymbol{\Lambda}} \begin{bmatrix} \boldsymbol{\eta}_{1,i} \\ \boldsymbol{\zeta}_{1,i} \end{bmatrix} + \boldsymbol{\epsilon}_{1,i} = \underbrace{\begin{bmatrix} 7 & 5 & 6 & 10 & 21 \\ 6 & 6 & 7 & 12 & 18 \\ 6 & 9 & 4 & 18 & 18 \\ 5 & 5 & 6 & 10 & 15 \\ 4 & 6 & 6 & 12 & 12 \end{bmatrix}}_{\tilde{\boldsymbol{\Lambda}}} \underbrace{\begin{bmatrix} \tilde{\boldsymbol{\eta}}_{1,i} \\ \tilde{\boldsymbol{\zeta}}_{1,i} \end{bmatrix}}_{\tilde{\boldsymbol{\Lambda}}\tilde{\mathbf{A}}_1} + \boldsymbol{\epsilon}_{1,i}, \quad (6)$$

$$\mathbf{Y}_{2,i} = \underbrace{\begin{bmatrix} 7 & 5 & 6 & 10 & 24 \\ 6 & 6 & 7 & 12 & 28 \\ 6 & 9 & 4 & 18 & 16 \\ 5 & 5 & 6 & 10 & 24 \\ 4 & 6 & 6 & 12 & 24 \end{bmatrix}}_{\boldsymbol{\Lambda}} \underbrace{\begin{bmatrix} \boldsymbol{\eta}_{2,i} \\ \boldsymbol{\zeta}_{2,i} \end{bmatrix}}_{\boldsymbol{\Lambda}\mathbf{A}_2} + \boldsymbol{\epsilon}_{2,i} = \underbrace{\begin{bmatrix} 7 & 5 & 6 & 10 & 24 \\ 6 & 6 & 7 & 12 & 28 \\ 6 & 9 & 4 & 18 & 16 \\ 5 & 5 & 6 & 10 & 24 \\ 4 & 6 & 6 & 12 & 24 \end{bmatrix}}_{\tilde{\boldsymbol{\Lambda}}} \underbrace{\begin{bmatrix} \tilde{\boldsymbol{\eta}}_{2,i} \\ \tilde{\boldsymbol{\zeta}}_{2,i} \end{bmatrix}}_{\tilde{\boldsymbol{\Lambda}}\tilde{\mathbf{A}}_2} + \boldsymbol{\epsilon}_{2,i}. \quad (7)$$

That the above equations can each be written in two equivalent decompositions illustrates the *information switching* problem: we cannot distinguish whether the column  $\boldsymbol{\Lambda} \times [0 \ 2 \ 0]^T = [10 \ 12 \ 18 \ 10 \ 12]^T$  is a part of the shared effect or the study-specific effect. Although the  $\mathbf{A}_s$  matrices should take into account the study-specific variations only, the individual effect of one study in this example can be at least “partially explained” by the others. From the perspective of the statistical model,  $\mathbf{A}_s$ ’s are no longer study-specific, but absorb a part of the shared variation which should be captured entirely by  $\boldsymbol{\Lambda}$ . In Section 2.1.1 we identify the necessary and sufficient condition causing this issue and propose an *almost sure* solution.

Rotational ambiguity has been well documented in the prior literature, affecting

both MSFA and PFA. In addition, MSFA suffers from information switching—briefly, for a  $d \times d$  order symmetric matrix  $\tilde{\mathbf{C}}$  such that  $\Lambda\Lambda^T - \tilde{\mathbf{C}} \succ \mathbf{0}$ ,  $\Phi_s\Phi_s^T + \tilde{\mathbf{C}} = \tilde{\Phi}_s\tilde{\Phi}_s^T$  for some  $d \times q_s$  order matrix  $\tilde{\Phi}_s$ . To resolve this, [De Vito et al. \(2019\)](#) restrict the augmented matrix  $[\Lambda \ \Phi_1 \ \dots \ \Phi_S]$  to be lower-triangular. Doing so incurs the tradeoff of introducing an order dependence ([Frühwirth-Schnatter and Lopes, 2018](#)); when no natural ordering exists, results can be very sensitive to permutations of the variables or studies ([Carvalho et al., 2008](#)). These structural constraints also can affect mixing and yield inconsistent estimates ([Millsap, 2001](#); [Erosheva and Curtis, 2017](#)). On the other hand, [Roy et al. \(2021\)](#) set  $\mathbf{Q}_1 = \mathbf{I}_d$  to impose identifiability in PFA, which can again be sensitive to the choice of the “first” study. In the following section, we provide *almost sure* solutions to the identifiability issues under much milder conditions, avoiding any such structural assumptions.

### 2.1.1 Resolving Information Switching

We now derive the necessary and sufficient conditions for information switching.

**Lemma 1.** *Assume that the data admits the marginal distribution in (2) for all the studies. Then information switching occurs if and only if there exists  $\Lambda$  and  $\mathbf{A}_s$ s such that  $\mathbf{Y}_{s,i} \stackrel{\text{iid}}{\sim} N_d(\mathbf{0}, \Lambda\Lambda^T + \Lambda\mathbf{A}_s\mathbf{A}_s^T\Lambda^T + \Delta)$  and  $\bigcap_{s=1}^S \mathbb{C}(\mathbf{A}_s)$  is non-null, where  $\mathbb{C}(\mathbf{A})$  denotes the column space of a matrix  $\mathbf{A}$ .*

Intuitively, a non-null  $\bigcap_{s=1}^S \mathbb{C}(\mathbf{A}_s)$  implies that the  $\mathbf{A}_s$  matrices are no longer study-specific. As we saw in example (5),  $\mathbf{A}_s$  can absorb a part of the shared variation which is meant to be captured by  $\Lambda$ . The Lemma provides requisite insights to avoid this with a very simple condition to ensure  $\Lambda$  fully explains the shared covariance.

**Theorem 1.** *If  $\sum_{s=1}^S q_s \leq q$  then information switching has zero support under any non-degenerate continuous prior on  $\mathbf{A}_s$ .*

Intuitively, aggregating multiple data views is a fruitful pursuit only when the datasets share enough similarity or structure; it is natural to expect that our subspace factor model is well-posed when there are fewer study-specific latent factors than shared factors. Theorem 1 makes this intuition precise, showing that the potential problem of information switching is resolved *almost surely*—under any continuous prior on  $\mathbf{A}_s$ —as long as  $\sum_{s=1}^S q_s \leq q$ . The assumption is therefore a natural one, and  $\Sigma$  is completely identifiable as a result, allowing for us to study and interpret the interaction between variables. To illustrate concretely in the context of the above example, consider setting the shared  $\tilde{\Lambda}$  to be a  $5 \times 4$  matrix and  $q_1 = q_2 = 1$ , i.e. right-hand side of (6)-(7). Now,  $\tilde{\Lambda}$  accounts for the variability in the marginal distribution (2), and in turn the parts explained by  $\mathbf{A}_1$  and  $\mathbf{A}_2$  no longer have intersection. Notably, the strategy of restricting the augmented matrix  $[\Lambda \ \Phi_1 \ \dots \ \Phi_S]$  to be lower-triangular by [De Vito \*et al.\* \(2019\)](#) also requires a similar condition  $q + \sum_{s=1}^S q_s \leq d$ , but is affected by the problem of order-dependence.

### 2.1.2 Resolving Rotational Ambiguity

Identifiability with respect to orthogonal rotation (II) is not essential for estimating the shared covariance  $\Sigma$ , since  $\Lambda \Lambda^T$  remains identifiable. However, rotational ambiguity does create obstacles to inferring interpretable lower-dimensional factors ([Russell, 2002](#); [Iacob \*et al.\*, 2016](#)). To avoid order dependence arising from structural assumptions, it is common to address the issue via post-processing the samples ([Legramanti \*et al.\*, 2020](#); [Roy \*et al.\*, 2021](#); [De Vito \*et al.\*, 2021](#); [Papastamoulis and Ntzoufras, 2022](#), and others).

Interpretability of the factor loadings is greatly enhanced by sparsity—for example, the sparse subset of genes with nonzero loadings onto a common factor can be

associated with a common biological pathway. Even when one places a shrinkage prior on the loadings to favor (near) sparsity, this desired structure is potentially destroyed after applying post-processing algorithms to the MCMC samples of the loadings. To avoid this, we adopt the approach of [Poworoznek \*et al.\* \(2021\)](#). The method first tackles the generic rotational invariance across the MCMC samples using an *orthogonalization step* leveraging the varimax transformation ([Kaiser, 1958](#)) to resolve ambiguity up to switching of the column labels and signs. These ambiguities are both resolved in the next step by *matching* each MCMC sample to a reference matrix called a *pivot*, aligning samples via a greedy maximization scheme.

The post-processed MCMC samples can thus be considered *matched and aligned* with respect to a common orthogonal transformation for inference downstream. Critically, the varimax rotation in the *orthogonalization step* implicitly induces sparsity ([Rohe and Zeng, 2020](#)). In more detail, the varimax criterion is given by

$$\mathbf{H}_{\text{VARIMAX}} = \arg \max_{\mathbf{H}} \left[ \frac{1}{d} \sum_{h=1}^q \sum_{j=1}^d (\mathbf{\Lambda} \mathbf{H})_{j,h}^4 - \sum_{h=1}^q \left\{ \frac{1}{d} \sum_{j=1}^d (\mathbf{\Lambda} \mathbf{H})_{j,h}^2 \right\}^2 \right],$$

and describes the optimal rotation maximizing the sum of the variances of squared loadings. Intuitively, this is achieved if (i) any given variable has a high loading on a single factor but near-zero loadings on the others, and (ii) any given factor is constituted by a few variables with very high loadings but near-zero support from the others. As a result, the summary matrix obtained from the posterior MCMC samples of  $\mathbf{\Lambda}$  is sparse upon applying varimax rotation, while the marginal distribution of the data is unaffected. Section [S.4.2](#) of the supplementary materials contains thorough simulations showing that this strategy accurately recovers  $\mathbf{\Lambda}$  consistently across several realistic scenarios. As  $\mathbf{\Lambda}^{(s)} = \mathbf{\Lambda} \mathbf{A}_s$  can be defined to denote the study-specific loading matrices, the above prescription applies similarly to obtaining study-specific loadings from samples of  $\mathbf{\Lambda}^{(s)}$ .

## 2.2 Latent Dimensions and Prior Specification

**Latent Dimensions:** In most practical applications, we do not know the column dimensions of  $\Lambda$  and  $\mathbf{A}_s$ , denoted  $q$  and  $q_s$  respectively. Although one could choose priors on  $q$  and  $q_s$  and implement reversible-jump algorithms (Green, 1995), this will often lead to inefficient computation, particularly in large  $d$  cases. Instead, it has become common practice in the single-study literature to use overfitted factor models by first fixing  $q$  at some upper bound and then leveraging appropriate priors to shrink the extra columns (Legramanti *et al.*, 2020; Schiavon *et al.*, 2022, and related others). This strategy substantially simplifies MCMC implementations. To choose upper bounds on the number of factors in practice, we employ augmented implicitly restarted Lanczos bidiagonalization (Baglama and Reichel, 2005) to obtain approximate singular values and eigenvectors of the pooled dataset, choosing the smallest  $\hat{q}$  that explains at least 95% of the variability in the data. After doing so, the simple choice  $\hat{q}_s = \hat{q}/S$  satisfies the conditions in Theorem 1. We later show in Section 3 that recovering the marginal covariance is asymptotically robust with respect to the choice of  $q$  and  $q_s$  under appropriate priors on  $\Lambda$ .

**Prior Specifications:** In high-dimensional applications, it is important to reduce the number of parameters in the factor loadings matrices for statistical efficiency in estimating the shared and study-specific contributions to the large covariance matrix. Among a wide variety of appropriate shrinkage priors, we use the Dirichlet-Laplace (DL, Bhattacharya *et al.*, 2015) for its near-minmax optimal contraction rates in the single-study context (Pati *et al.*, 2014) and computational simplicity. We let  $\text{vec}(\Lambda) \sim \text{DL}(a)$  where  $a$  is a suitably chosen hyperparameter; details appear in Section S.1 of the supplementary materials. For the study-specific terms  $\mathbf{A}_s$ , we let its entries  $a_{s,i,j} \stackrel{\text{iid}}{\sim} N(0, b_{\mathbf{A}})$ , a choice that avoids information switching *almost surely*.

Regarding the residual variances, we consider  $\log \delta_j^2 \stackrel{\text{iid}}{\sim} N(\mu_\delta, \sigma_\delta^2)$  as log-normal distributions have modes bounded away from zero and tend to produce more numerically stable estimates compared to commonly used inverse-gamma and half-Cauchy priors (Gelman, 2006).

### 3 Posterior Contraction Rates

We now analyze the posterior contraction rates for recovering the shared and study-specific covariance matrices. Before detailing the assumptions on the true data-generating mechanism and the postulated SUFA model, we fix notational conventions. We let  $\Pi_n(\cdot)$  denote the prior and  $\Pi_n(\cdot | \mathcal{D}_n)$  the corresponding posterior given data  $\mathcal{D}_n = \{\mathbf{Y}_{1,1}, \dots, \mathbf{Y}_{1,n_1}, \dots, \mathbf{Y}_{S,1}, \dots, \mathbf{Y}_{S,n_S}\}$ . Throughout,  $\|\mathbf{A}\|_F$  and  $\|\mathbf{A}\|_2$  denote the Frobenius and spectral norms of a matrix  $\mathbf{A}$ , respectively. For real sequences  $\{a_n\}$ ,  $\{b_n\}$ ,  $a_n = o(b_n)$  implies that  $\lim |a_n/b_n| = 0$  and  $a_n \succ b_n$  implies that  $\liminf a_n/b_n > 0$ . A  $d$ -dimensional vector  $\boldsymbol{\theta}$  is said to be  $s$ -sparse if it has only  $s$  nonzero elements, and we denote the set of all  $s$ -sparse vectors in  $\mathbb{R}^d$  by  $\ell_0[s, d]$ .

**Data-generating mechanism:** We assume that the data are generated according to  $\mathbf{Y}_{s,1:n_s} \stackrel{\text{iid}}{\sim} N_{d_n}(\mathbf{0}, \boldsymbol{\Sigma}_{0sn})$  for each study  $s = 1, \dots, S$ . Here,  $\boldsymbol{\Sigma}_{0sn} = \boldsymbol{\Lambda}_{0n}\boldsymbol{\Lambda}_{0n}^T + \boldsymbol{\Lambda}_{0n}\mathbf{A}_{0sn}\mathbf{A}_{0sn}^T\boldsymbol{\Lambda}_{0n}^T + \boldsymbol{\Delta}_{0n}$  with  $\boldsymbol{\Lambda}_{0n}$  a  $d_n \times q_{0n}$  sparse matrix,  $\mathbf{A}_{0sn}$  a  $q_{0n} \times q_{0sn}$  matrix with real entries, and  $\boldsymbol{\Delta}_{0n} := \text{diag}(\delta_{01}^2, \dots, \delta_{0d_n}^2)$ . Compared to the setup in prior work by Pati *et al.* (2014), we consider multiple studies and allow heterogeneous residual errors, which will provide more realism in modeling the data as well as require a more nuanced analysis. Denoting  $n = \sum_{s=1}^S n_s$  the combined sample size across studies, we will allow the model parameters to increase in dimension with  $n$  as suggested by the subscripts in our notations. Under this setup, we now state the required sparsity conditions on the true parameters in order to recover the shared as well as the study

specific covariance structures in high-dimensional settings.

- (C1) For  $s = 1, \dots, S$ ,  $\liminf_{n \rightarrow \infty} \frac{n_s}{n} > 0$ .
- (C2) Let  $\{q_{0n}\}$ ,  $\{q_{0sn}\}$  for  $s = 1, \dots, S$ ,  $\{s_n\}$  and  $\{d_n\}$  be increasing sequences of positive integers and  $\{c_n\}$  be an increasing sequence of positive real numbers such that  $\sum_{s=1}^S q_{0sn} \leq q_{0n} < d_n$ .
- (C3)  $\Lambda_{0n}$  is a  $d_n \times q_{0n}$  full rank matrix such that each column of  $\Lambda_{0n}$  belongs to  $\ell_0[s_n, d_n]$ ,  $\|\Lambda_{0n}\|_2^2 = o(\frac{c_n}{q_{0n}})$  and  $\max_{1 \leq s \leq S} \|\Lambda_{0sn}\|_2^2 = o(q_{0n})$ .
- (C4)  $\max_j \delta_{0d_n}^2 = o(c_n)$  and  $\min_j \delta_{0d_n}^2 > \delta_{\min}^2$  where  $\delta_{\min}^2$  is a positive constant.
- (C5)  $\frac{d_n \max\{(\log c_n)^2, \log d_n\}}{c_n^2 s_n q_{0n} \log(d_n q_{0n})} = o(1)$ .

In less technical terms, (C1) ensures that none of the studies has a negligible proportion of the data. (C2) and (C3) specify the requisite sparsity conditions. Together, (C3) and (C4) imply that the marginal variances grow in  $o(c_n)$  while ensuring that they are also bounded away from 0. The technical condition (C5) specifies the relative rate of increment of the parameters.

**Specifics of the posited SUFA model:** In practice, the latent dimensions are unknown, and it is desirable to establish theory for the strategy of overspecifying a model and then shrinking redundant parameters via shrinkage priors. This section identifies conditions under which we may derive guarantees in this overparametrized setting. To this end, let  $\mathbf{Y}_{s,1:n_s} \stackrel{\text{iid}}{\sim} N_{d_n}(\mathbf{0}, \Lambda_n \Lambda_n^T + \Lambda_n \mathbf{A}_{sn} \mathbf{A}_{sn}^T \Lambda_n^T + \Delta_n)$  where  $\Lambda_n$  and  $\mathbf{A}_{sn}$  are  $d_n \times q_n$  and  $q_n \times q_{sn}$  matrices, respectively, and  $\Delta_n = \text{diag}(\delta_1^2, \dots, \delta_{d_n}^2)$ . The parameters in the posited (possibly misspecified) model do not have 0 subscripts, to distinguish from their ground truth counterparts.

We let  $\{q_n\}$ ,  $\{q_{sn}\}$  be increasing sequences of positive integers such that  $q_{0n} \leq q_n$ ,  $q_{0sn} \leq q_{sn}$  so that the chosen number of shared and study-specific latent factors upper bound the respective true (also unknown) numbers resulting in a misspeci-

fied and over-parametrized factor model in the postulation. We additionally assume  $\sum_{s=1}^S q_{sn} \leq q_n$  to ensure the identifiability condition from Theorem 1. As discussed in Section 2.2 we let  $\text{vec}(\boldsymbol{\Lambda}_n) \sim \text{DL}(a_n)$  with  $a_n = 1/d_n q_n$  to impose sparsity on  $\boldsymbol{\Lambda}_n$ . Below, we provide sufficient conditions on the overspecified dimensions to ensure consistency of the class of postulated models even when they are misspecified.

(D1)  $q_n^2 = o(c_n^2 s_n q_{0n})$  and  $\lim_{n \rightarrow \infty} \frac{c_n^{12}}{n} \{s_n q_{0n} \log(d_n q_n)\}^3 = 0$ .

(D2)  $\log(d_n q_n) \min \left\{ \frac{c_n}{s_n q_{0n}^3} (d_n q_n)^{c_n^2}, s_n (d_n q_n)^{\frac{c_n^2}{q_n^2} s_n q_{0n}}, \frac{s_n q_{0n}}{(\log c_n)^2} (d_n q_n)^{\frac{c_n^2}{d_n} s_n q_{0n}} \right\} \succ n$ .

The first condition (D1) makes explicit how much overparametrization can be tolerated, while the second condition specifies the signal-to-noise ratio. The second condition in (D1) and (C5) jointly imply that  $d_n \log d_n$  grows in  $o(n^\alpha)$  for some  $0 < \alpha < 1$ . (D2) can be interpreted as a lower bound on the signal strength in order to recover the covariance structures from the data.

**Contraction results:** Let  $\boldsymbol{\Theta}_{0n} = \{\boldsymbol{\Lambda}_{0n}, \boldsymbol{\Delta}_{0n}, \mathbf{A}_{01n}, \dots, \mathbf{A}_{0Sn}\}$  be the true data-generating parameters and  $\mathbb{P}_{0n}$  denote the joint distribution of  $\mathcal{D}_n$  under  $\boldsymbol{\Theta}_{0n}$ . We define  $\boldsymbol{\Sigma}_{0n} = \boldsymbol{\Lambda}_{0n} \boldsymbol{\Lambda}_{0n}^T + \boldsymbol{\Delta}_{0n}$  as the true shared covariance structure and  $\boldsymbol{\Sigma}_n = \boldsymbol{\Lambda}_n \boldsymbol{\Lambda}_n^T + \boldsymbol{\Delta}_n$  to be the shared covariance in the postulated model. The following result formally characterizes the posterior contraction properties around  $\boldsymbol{\Sigma}_{0n}$ .

**Theorem 2** (Contraction rate). *For any  $\boldsymbol{\Theta}_{0n}$  satisfying (C1)-(C5) and priors satisfying (D1)-(D2), we have  $\mathbb{E}_{\mathbb{P}_{0n}} \lim_{n \rightarrow \infty} \Pi_n (\|\boldsymbol{\Sigma}_n - \boldsymbol{\Sigma}_{0n}\|_2 > M \varepsilon_n \mid \mathcal{D}_n) = 0$ , where  $\varepsilon_n = c_n^6 \sqrt{\frac{\{s_n q_{0n} \log(d_n q_n)\}^3}{n_1 + \dots + n_S}}$  and  $M > 0$  is a large enough constant.*

Theorem 2 has several important implications for modeling and computation. First, the combined sample size appears in the denominator of the contraction rate  $\varepsilon_n$ , which is consistent with the intuition that learning the shared covariance structure improves inference by borrowing strength across multiple studies or data views. Because the true values of  $q_{0n}$  and  $q_{0sn}$  are unknown, we made the weak assumption

that the specified column dimensions are larger than the ground truth dimensions. Although the best contraction rate is unsurprisingly achieved when correctly setting  $q_n = q_{0n}$ , Theorem 2 validates the practice of beginning with overparametrized models, showing that it is still possible to recover  $\Sigma_{0n}$ . This result provides an important theoretical foundation to the common heuristic strategy of setting the column dimension of  $\Lambda$  to some upper bound in FA model implementations.

Note that  $\Lambda_{0n}\mathbf{A}_{0sn}\mathbf{A}_{0sn}^T\Lambda_{0n}^T$ s are the study-specific covariance structures. The following result shows that these study-specific terms can also be recovered for all  $s$ .

**Corollary 1** (Recovering individual structures). *Under the same conditions as Theorem 2,  $\lim_{n \rightarrow \infty} \mathbb{E}_{\mathbb{P}_{0n}} \Pi_n \left( \|\Lambda_n \mathbf{A}_{sn} \mathbf{A}_{sn}^T \Lambda_n^T - \Lambda_{0n} \mathbf{A}_{0sn} \mathbf{A}_{0sn}^T \Lambda_{0n}^T\|_2 > M\varepsilon_n \mid \mathcal{D}_n \right) = 0$ .*

## 4 Gradient-based Posterior Computation

Gibbs sampling is the most popular approach for posterior inference in Bayesian factor models. While such an approach is straightforward for our model (1), it is well known that alternately updating latent factors and covariance structure parameters can lead to slow mixing. In addition, instantiating the latent factors  $\boldsymbol{\eta}_{s,i}$  and  $\boldsymbol{\zeta}_{s,i}$  quickly increases computational cost for large samples. It has been observed that marginalizing out auxiliary parameters can often dramatically improve MCMC performance (Robert and Roberts, 2021). In view of this, we develop a Hamiltonian Monte Carlo (HMC, Neal, 2011) within Gibbs sampler that makes use of the marginal posterior, after integrating out all latent factors. The HMC sampler makes smarter proposals utilizing the gradient of the log-target density. We will see that our proposed algorithm confers substantial gains in real computation times compared to standard Gibbs approaches.

Denote the log-likelihood of the marginal SUFA model (2) by  $\mathcal{L} := K -$

$\frac{1}{2} \sum_{s=1}^S \{n_s \log |\Sigma_s| + \text{trace}(\Sigma_s^{-1} \mathbf{W}_s)\}$  with marginal covariance matrix  $\Sigma_s = \Lambda(\mathbf{I}_q + \mathbf{A}_s \mathbf{A}_s^T) \Lambda^T + \Delta$ , sample sum of squares matrix  $\mathbf{W}_s = \sum_{i=1}^{n_s} \mathbf{Y}_{s,i} \mathbf{Y}_{s,i}^T$  for study  $s$  and a constant  $K$ . The DL prior on  $\Lambda$  admits a Gaussian distribution conditionally on the hyperparameters  $\tau$ ,  $\psi$  and  $\phi$  (see (S.1) in the supplementary materials for details). Thus from the prior specifications outlined in Section 2.2, the posterior density of  $\Theta := (\Lambda, \Delta, \mathbf{A}_1, \dots, \mathbf{A}_S)$  given  $\psi, \phi, \tau$  and the observed data is given by

$$\Pi(\Theta | -) = \exp(\mathcal{L}) \times \Pi(\Lambda | \tau, \phi, \psi) \times \Pi(\Delta) \times \prod_{s=1}^S \Pi(\mathbf{A}_s). \quad (8)$$

To implement HMC, gradients of  $\log \Pi(\Theta | -)$  with respect to  $\Theta$  are required (see Section S.3 in the supplementary materials for a general discussion on HMC algorithms). In Section A.2 of the Appendix we show that the gradients can be analytically expressed. Equipped with these expressions, we propose an HMC-within-Gibbs sampler where  $\Theta$  is updated given  $(\tau, \phi, \psi)$  using an HMC step, and then the hyperparameters  $(\tau, \phi, \psi)$  are updated conditionally on  $\Lambda$  using a Gibbs step following [Bhattacharya et al. \(2015\)](#). The vanilla HMC algorithm requires the following tuning parameters: a positive real number  $\delta t$ , a positive integer  $L$  and a positive definite matrix  $\mathbf{M}$  of the same order as  $\Theta$ . Letting  $\nabla V(\Theta) = -\frac{\partial}{\partial \Theta} \log \Pi(\Theta | -)$  be the gradient of the negative log-posterior, we outline the HMC-within-Gibbs sampler in Algorithm 1 to obtain  $N$  MCMC samples from the joint posterior distribution of  $(\Theta, \tau, \psi, \phi)$ . Implementing Algorithm 1 requires computing  $\log \Pi(\Theta | -)$  as well as  $\frac{\partial}{\partial \Theta} \log \Pi(\Theta | -)$  at each MCMC step. In Section A.2 of the Appendix we show that these quantities can be computed very efficiently by distributing the calculations over parallel processes.

Before validating theory and methods in empirical studies, we highlight two advantages of our sampler. First, it can be adapted to any prior with (conditionally) differentiable density, including the spike-and-slab ([Ishwaran and Rao, 2005](#)), spike-and-slab lasso ([Ročková and George, 2016](#)), horseshoe ([Carvalho et al., 2009](#)),

multiplicative gamma (Bhattacharya and Dunson, 2011), generalized double Pareto (Armagan *et al.*, 2013), cumulative shrinkage (Legramanti *et al.*, 2020), and others. Almost all of these admit a conditionally Gaussian prior on  $\Lambda$ , so that adapting Algorithm 1 requires only modifying the Gibbs step. Second, a crucial advantage of Algorithm 1 is its scalability with respect to the sample size. In particular, the log-likelihood  $\mathcal{L}$  and its gradient depend on the data only through the study-specific sample sum of squares  $\mathbf{W}_s$ , which just needs to be computed and cached once.

## 5 Empirical Study

### 5.1 Simulated Experiments

To assess the proposed methodology, we generate synthetic data according to the true model (3) under three scenarios induced by different  $\Lambda$  matrices. The ground truth shared covariance structures are displayed in the first column of Figure 2; complete

---

#### Algorithm 1: HMC-within-Gibbs Sampler for SUFA

---

```

1 Initialize  $\Theta$ ,  $\psi$ ,  $\phi$  and  $\tau$ .
2 for  $i = 1, \dots, N$  do
    HMC Update  $\Theta$ : Draw  $\mathbf{p} \sim N(\mathbf{0}, \mathbf{M})$  and initiate  $\{\Theta(0), \mathbf{p}(0)\} = (\Theta_{i-1}, \mathbf{p})$ . Repeat the
    following  $L$  leapfrog steps to numerically solve Hamiltonian equations:
    for  $\ell = 0, \dots, L-1$  do
         $\Theta\{t + (\ell + 1)\delta t\} = \Theta(t + \ell\delta t) + \delta t \mathbf{M}^{-1} [\mathbf{p}(t + \ell\delta t) - \frac{\delta t}{2} \nabla V\{\Theta(t + \ell\delta t)\}]$ ,
         $\mathbf{p}\{t + (\ell + 1)\delta t\} = \mathbf{p}(t + \ell\delta t) - \frac{\delta t}{2} [\nabla V\{\Theta(t + \ell\delta t)\} + \nabla V\{\Theta(t + (\ell + 1)\delta t)\}]$ .
    end
    Letting  $(\Theta', \mathbf{p}') = (\Theta(t + L\delta t), \mathbf{p}(t + L\delta t))$ , set  $\Theta_i = \Theta'$  with probability
     $\min \left\{ 1, e^{H(\Theta', \mathbf{p}') - H(\Theta_{i-1}, \mathbf{p})} \right\}$ , where  $H(\Theta, \mathbf{p}) = -\log \Pi(\Theta | -) + \mathbf{p}^T \mathbf{M}^{-1} \mathbf{p} / 2$ .
    Gibbs Update  $\psi$ ,  $\phi$  and  $\tau$ :
    (i) For  $j = 1, \dots, d$  and  $h = 1, \dots, q$  sample  $\tilde{\psi}_{j,h}$  independently from inverse-Gaussian
        distributions  $iG(\tau_{i-1} \phi_{i-1,j,h} / |\lambda_{i,j,h}|, 1)$  and set  $\psi_{i,j,h} = 1 / \tilde{\psi}_{j,h}$ .
    (ii) Draw  $T_{j,h}$  independently from a generalized inverse Gaussian distributions
         $giG(a - 1, 1, 2|\lambda_{i,j,h}|)$  and set  $\phi_{i,j,h} = T_{j,h} / T$  with  $T = \sum_{j,h} T_{j,h}$ .
    (iii) Sample  $\tau_i \sim giG \left\{ dq(1 - a), 1, 2 \sum_{j,h} \frac{|\lambda_{i,j,h}|}{\phi_{i,j,h}} \right\}$ .
3 end

```

---

details of the simulation setup and further figures appear in Section S.4.1 of the supplementary materials. For each scenario, we also examine performance under two misspecified settings: (i) *slight misspecification*, where  $\Phi_s = \Lambda \mathbf{A}_s + \mathbf{E}_s$  and  $\mathbf{E}_s$  is a matrix of randomly generated errors, and (ii) *complete misspecification*, where  $\Phi_s$  is independent of  $\Lambda$  for each study  $s = 1, \dots, S = 5$ . We vary  $d = 50, 200$ , and  $450$  and set  $n_s = \text{Poisson}(50/S)$ ,  $\text{Poisson}(200/S)$  and  $\text{Poisson}(400/S)$ , respectively, for each  $s = 1, \dots, S$ . We generate  $q_s \sim \min\{1, \text{Poisson}(q/S)\}$  where  $q = 10$  for the  $d = 50$  case and  $q = 20$  otherwise. Finally, we repeat all experiments over 25 trials.

**Peer methods:** We compare the performance of our proposed SUFA model with B-MSFA (De Vito *et al.*, 2021) and PFA (Roy *et al.*, 2021). However, PFA did not scale beyond  $d > 50$  and therefore we could only apply it for  $d = 50$ . Both of these methods use the multiplicative gamma process prior (Bhattacharya and Dunson, 2011) on  $\Lambda$  and available code requires the user to input an upper bound on the number of latent factors; we choose the bound following the strategy in Section 2.2.

To assess model fit, we consider the *widely applicable Bayesian information criterion* (WBIC, Watanabe, 2013), with lower values implying better fit. Boxplots of the WBIC values across independent replicates are shown in the top panel of Figure 1. For  $d = 50$ , PFA performs slightly better than SUFA only in the completely misspecified case. As dimension grows, performance improvements under SUFA become more evident. Identifiability issues with B-MSFA may degrade parameter estimation performance but are not expected to adversely impact goodness-of-fit measures such as WBIC. As SUFA was motivated by improving identifiability, the better model fit is surprising, and may be explained by (i) better borrowing of information as discussed in Section 2.1, (ii) more effective use of the sparsity in  $\Lambda$  induced through the DL prior, and (iii) more efficient posterior sampling using the proposed HMC-within-

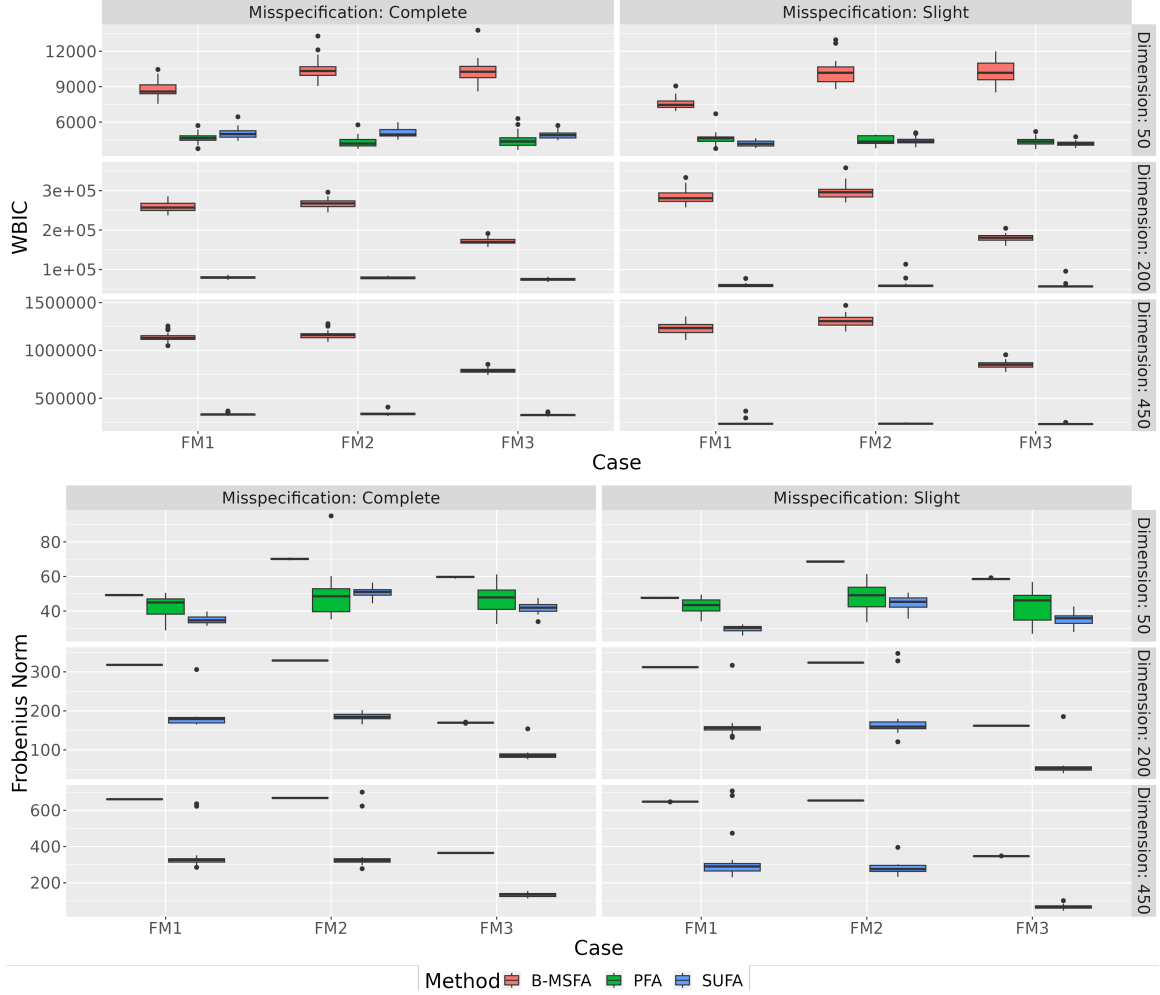


Figure 1: Comparing our proposed SUFA with B-MSFA and PFA across different simulation scenarios and dimensions: The top panel shows the boxplots of the WBIC values and the middle panel shows the boxplots of Frobenius norms between the true and estimated shared covariance structure  $\Sigma$ .

Gibbs sampler (itself in part due to improved parameter identifiability).

We compute the Frobenius norms between the simulation truth and estimated values of the shared covariance matrix  $\Sigma$ . Boxplots of the norms across independent replicates are shown in the bottom panel of Figure 1. In almost every case, SUFA yields the lowest estimation errors. In Figure 2, we plot the shared correlation matrices  $\mathbf{R} = \text{diag}(\Sigma)^{-\frac{1}{2}} \Sigma \text{diag}(\Sigma)^{-\frac{1}{2}}$  recovered by SUFA. In each setting, as a representative of the 25 independent replicates, we choose the one with the median

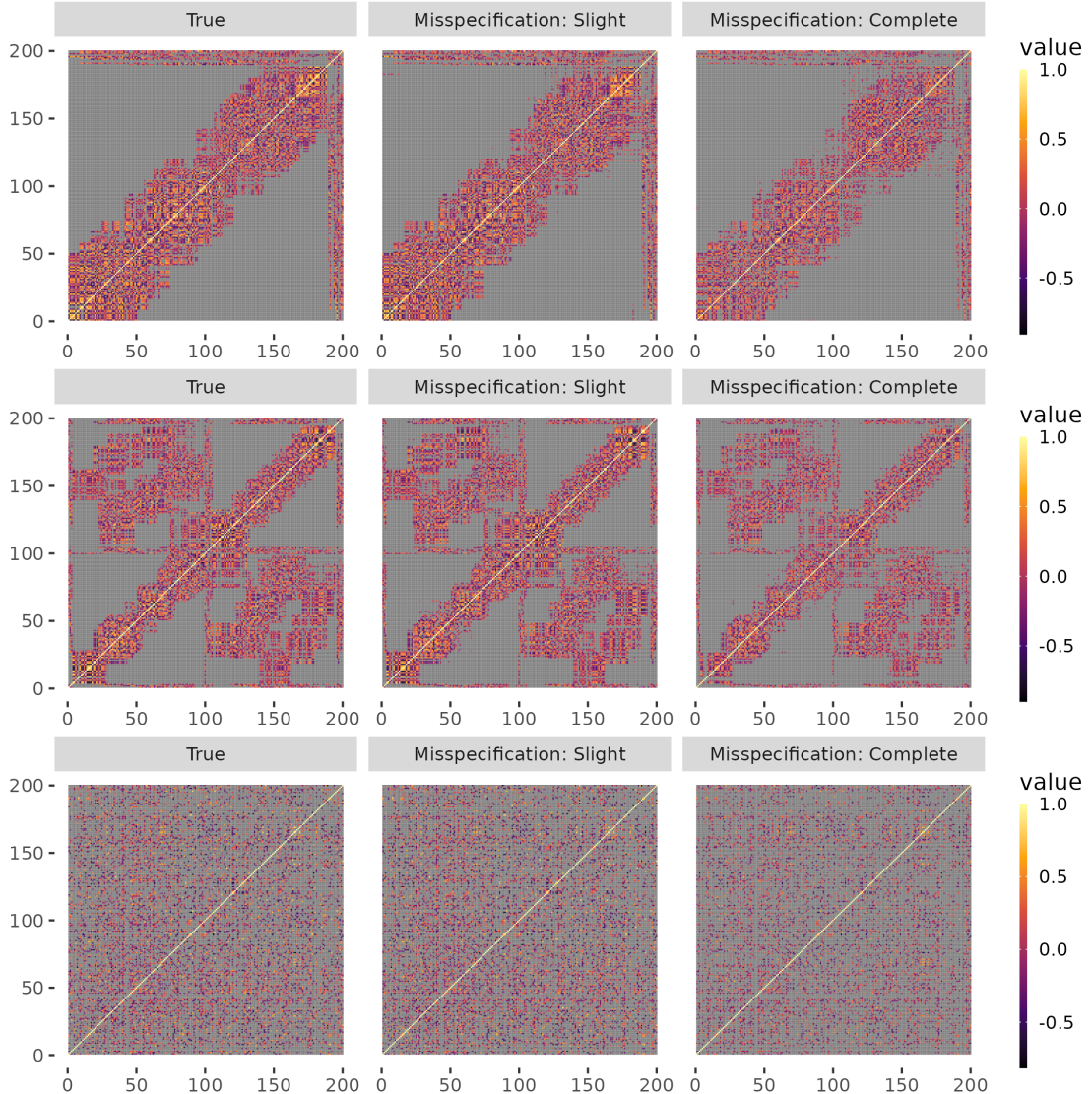


Figure 2: The true and estimated shared correlation matrix: horizontal panels correspond to the different factor models considered. In each panel, the true correlation matrix is shown in the leftmost plot; the middle and right plots are the point estimates in the slight and complete misspecified cases respectively.

Frobenius norm from the truth. We use the posterior mean across the MCMC samples as the point estimate. Due to page limits, we only show results for  $d = 200$  in Figure 2. For easier visualization of the correlation structure, in Figure 2 we use gray color for correlations having absolute value less than 0.10. The heatplots under the “True” panel of Figure 2 show the simulation truths of the three different correlation structures; the “Slight” and “Complete” misspecification panels show the recovered

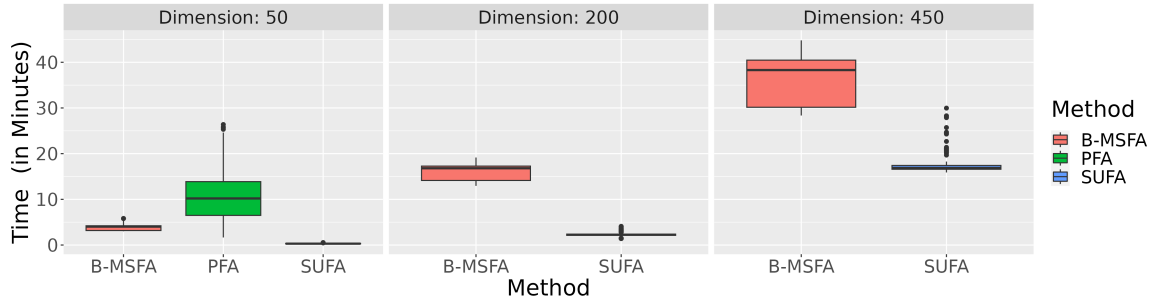


Figure 3: Comparing execution times (in Minutes) of B-MSFA, PFA and SUFA across increasing dimensions.

**R** by the SUFA model for the two model misspecification types under consideration. The figure clearly indicates that SUFA accurately recovers the shared correlation structures under misspecified scenarios as well. Additional favorable results on inferring the loadings  $\Lambda$  are included in Section S.4.2 of the supplementary materials. Finally, we compare the total runtimes for 7,500 MCMC iterations in Figure 3. PFA is slowest due to requiring updates of  $S$  dense  $d \times d$  matrices. However, owing to the distributed computing implementation of our HMC-within-Gibbs sampler, we observe dramatic improvements in computational efficiency using SUFA. Complete details of the parallelized implementation and a complexity analysis showing that each HMC step is of order  $\mathcal{O}(Lqd^2)$  appear in Section A.2 of the Appendix.

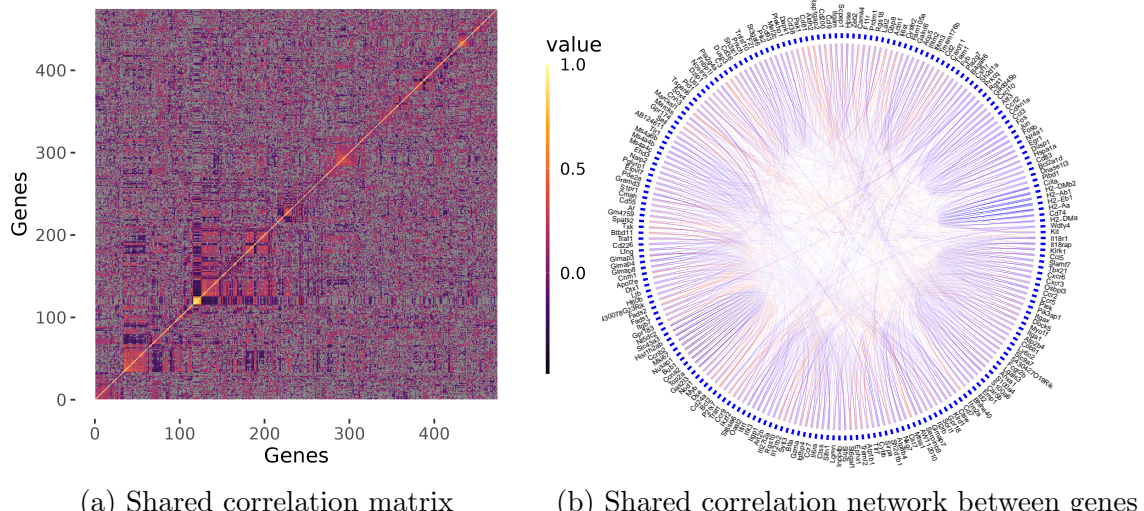
## 5.2 Application to Gene Expression Data

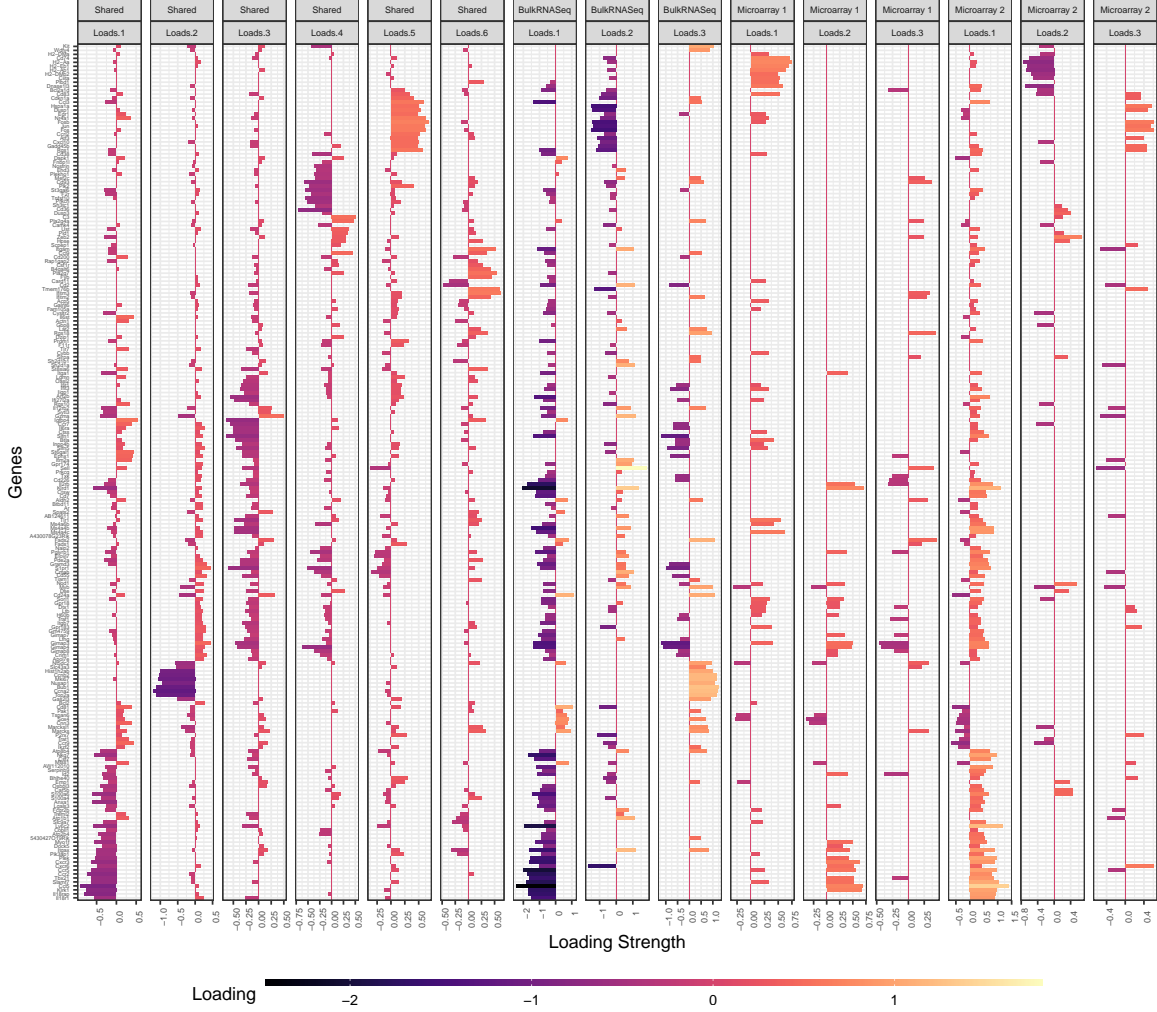
We now turn to a case study on gene associations among immune cells, which serve specialized roles in innate and adaptive immune responses that function to eliminate antigens (Gonzalez *et al.*, 2018). Understanding gene associations in immune cells is of particular current interest as an essential step in developing cancer therapeutics in immunotherapy (Tan *et al.*, 2020). Here, we integrate data from three studies analyzing gene expressions. The first is the GSE109125 bulkRNAseq dataset, collected from 103 highly purified immunocyte populations representing all lineages and sev-

eral differentiation cascades and profiled using the ImmGen pipeline (Yoshida *et al.*, 2019). The second study is a microarray dataset GSE15907 (Painter *et al.*, 2011; Desch *et al.*, 2011), measured on multiple *ex-vivo* immune lineages, primarily from adult B6 male mice. Finally, we include the GSE37448 (Elpek *et al.*, 2014) microarray dataset, also part of the Immgen project. After standard pre-processing (detailed in Section S.5.2 of the supplementary material), we work with 474 common genes measured on 156, 146 and 628 cells from the respective datasets.

We apply SUFA and B-MSFA to the integrated datasets, resulting in WBIC values of 424278 and 445916, respectively. This suggests that SUFA provides a better fit, and we hence focus on interpreting the SUFA results. First, we visualize the estimated shared correlation structure between genes in Figure 4(a). We use the uncertainty quantified by the posterior samples to infer whether correlations are zero—following common practice in the literature on Bayesian inference on sparsity patterns in covariance matrices (Ksheera Sagar *et al.*, 2021), we encode the off-diagonals of the correlation matrix as zero if the respective 95% posterior credible interval contains zero. This leads to a distinctive sparsity pattern.

Next, we focus on identifying important hub genes that have absolute correlation





(c) Shared and study-specific loading matrices

Figure 4: Results on ImmGen data: panel (a) shows the transpose of the shared loading matrix  $\Lambda$  and correlation matrix derived from  $\Sigma$  from left to right; panel (b) is the circos plot of the dependency structure between genes, blue (red) connection implies a positive (negative), their opacities being proportional to the corresponding association strengths. Associations are only plotted for absolute correlation  $\geq 0.25$ .

$\geq 0.25$  with at least 10 other genes. The resulting dependency network is summarized as a circos plot (Gu *et al.*, 2014) in Figure 4(b). Our findings are quite consistent with results from the prior literature: we observe strong positive correlation between the genes Ly6a, Ly6c1 and Ly6c2 identified within the murine Ly6 complex on chromosome 15 (Lee *et al.*, 2013); similar behavior is observed within the membrane-spanning 4A class of genes, namely Ms4a4c, Ms4a4b and Ms4a6b (Liang *et al.*, 2001). Bcl2a1b

and Bcl2a1d genes—two functional isoforms of the B cell leukemia 2 family member (Schenk *et al.*, 2017) also show strong positive correlations.

In addition to corroborating qualitative results in the prior literature with a principled statistical analysis, our study also reveals new insights via integrating the data. We find strong positive associations between genes Bub1, Ccna2, Ccnb2, Top2a, which corroborates findings from a study by Ashrafi *et al.* (2021) on adult human T cell leukemia. Interestingly, we find this group of genes strongly negatively correlated with those in the Gimap family, which are involved in lymphocyte development and play important roles in immune system homeostasis. On the other hand, the analysis reveals that the Gimap class features positive within-group associations, supporting recent studies that suggest Gimap proteins may interact with each other in roles such as moving cellular cargo along the cytoskeletal network (Limoges *et al.*, 2021). Up-regulation of the Ccr2 gene has been found to be associated with cancer advancement, metastasis and relapse (Hao *et al.*, 2020), whereas Ccr5 inhibitors exhibit negative association with lung metastasis of human breast cancer cell lines (Velasco-Velázquez *et al.*, 2012). Coherent with these studies, we find strong positive correlation between Ccr2 and Ccr5. We also observe Ccr2 to be highly positively correlated with Il18rap, supported by genome-wide association studies identifying their susceptibility with coeliac diseases (Amundsen *et al.*, 2010). Additionally we see strong positive association between the structurally related genes Il18rap and Il18r1 within the Il18 receptor complex (Pernet *et al.*, 1996). Interestingly, strong negative correlation is observed between the Il18 family of genes and the gene Cd81, which is required for multiple normal physiological functions (Levy, 2014). The joint analysis of multiple datasets using our SUFA framework thus reveals interesting findings adding to the relevant immunology literature, discovering potential relationships that warrant

further scientific study.

At a less detailed level, we visualize the top eight columns with highest sum-of-squares value from the shared loading matrix, and repeat for the top three columns of each study-specific loading matrix. These appear in Figure 4(c). The columns from the shared loading strongly indicate the existence of latent factors that govern the variability between correlated genes. Coherent with empirical studies (Wang *et al.*, 2014), the strongest signals appear in the bulkRNAseq data despite having much smaller sample size than the microarrays. The loadings of Microarray 2 show much stronger signals than those in Microarray 1, possibly due to the larger sample size of the former. These intuitive findings, corroborated by results from the prior literature, illustrate the interpretability of the learned study-specific loadings under SUFA.

## 6 Discussion

This article proposes a new factor analytic approach for covariance learning by integrating multiple related studies in high-dimensional settings. We provide practical solutions and theoretical guarantees for learning the shared covariance structure, resolving some long-standing identifiability issues in the literature. We also quantify the utility of data integration under the proposed model by way of improved learning rates with each additional study in our analysis of the posterior contraction properties. Finally, these contributions are developed alongside a scalable HMC approach to posterior inference capable of handing massive datasets. In thorough realistic simulation studies, we show that our proposed method outperforms several existing approaches in multiple aspects. Our approach yields new insights when applied to a gene network estimation problem, integrating immune cell gene expression datasets.

Leveraging low-rank matrix decompositions, factor models have widespread scope

in contemporary data analysis regimes beyond our focus on estimating covariance structure. These extensions include measurement error problems (Sarkar *et al.*, 2021), model-based clustering (Chandra *et al.*, 2023), conditional graph estimation (Chandra *et al.*, 2021), among many others. Our proposed SUFA approach can be readily adopted in these domains. Integrating data from multiple sources is of interest in many applications involving non-Gaussian data as well. Flexible copula-based factor models (Murray *et al.*, 2013; Lu *et al.*, 2017) can potentially handle such data. In the presence of multiple studies, our approach can be adopted using additional hierarchies in copula-based factor models. These extensions represent several examples of promising future directions building upon the ideas in this article, extending their scope beyond the problems we study here.

## Supplementary Materials

Complete prior specifications, proofs and details of the theoretical results and technical lemmas, extended simulation results, and details on the gene expression datasets.

## Acknowledgments

The authors are grateful for partial funding support from NIH grants R01-ES027498 and R01-ES028804, NSF grants DMS-2230074 and PIPP-2200047, and ERC Horizon 2020 grant agreement No. 856506.

## Appendix

### A.1 Proofs of Main Results

**Proof of Lemma 1.** We first show that information switching or the existence of a matrix  $\mathbf{C}$  as mentioned in (I) implies  $\bigcap_{s=1}^S \mathbb{C}(\mathbf{A}_s)$  is non-null. Since  $\mathbf{C}$  is symmetric,  $\mathbf{C} = \mathbf{H}\mathbf{D}\mathbf{H}^T$  where  $\mathbf{H} = [\mathbf{h}_1 \ \cdots \ \mathbf{h}_q]$  is an orthogonal matrix and  $\mathbf{D} =$

$\text{diag}(d_1, \dots, d_q)$  is a diagonal matrix with real entries. Clearly  $\mathbf{C} = \sum_{i=1}^q d_i \mathbf{h}_i \mathbf{h}_i^T$ . Letting  $\mathbf{C}^+ = \sum_{i=1}^q d_i \mathbb{1}_{d_i > 0} \mathbf{h}_i \mathbf{h}_i^T$  and  $\mathbf{C}^- = -\sum_{i=1}^q d_i \mathbb{1}_{d_i < 0} \mathbf{h}_i \mathbf{h}_i^T$ , we have  $\mathbf{C} = \mathbf{C}^+ - \mathbf{C}^-$ .

Let us first consider the case where  $\mathbf{C}^+ = \mathbf{0}$ . Since by assumption  $\mathbf{A}_s \mathbf{A}_s^T + \mathbf{C}$  is positive semi-definite (psd), for any non-zero vector  $\mathbf{x}$ ,  $\mathbf{x}^T (\mathbf{A}_s \mathbf{A}_s^T + \mathbf{C}) \mathbf{x} = 0$  for all  $s$  implies that  $\mathbf{x}^T \mathbf{C}^- \mathbf{x} = 0$ . Now for any psd matrix  $\mathbf{B}$  and non-zero vector  $\mathbf{x}$ ,  $\mathbf{x}^T \mathbf{B} \mathbf{x} = 0$  implies that  $\mathbf{x} \in \mathbb{N}(\mathbf{B})$  where  $\mathbb{N}(\mathbf{B})$  denotes the nullity of the column space of  $\mathbf{B}$ . Hence  $\mathbb{N}(\mathbf{A}_s) \subset \mathbb{N}(\mathbf{C}^-)$  for all  $s = 1, \dots, S$  implying that  $\mathbb{C}(\mathbf{C}^-) \subseteq \bigcap_{s=1}^S \mathbb{C}(\mathbf{A}_s)$ .

To complete the argument, we consider the case where  $\mathbf{C}^+$  is non-null. Note that  $\mathbf{I}_q - \mathbf{C} \succ \mathbf{0}$  implies that  $\mathbf{C}^+ \prec \mathbf{I}_q$  and therefore, without loss of generality, we can assume  $\mathbf{C}^- = \mathbf{0}$ . Henceforth we have  $\tilde{\mathbf{A}}_s \tilde{\mathbf{A}}_s^T = \mathbf{A}_s \mathbf{A}_s^T + \mathbf{C}^+$ . Redefine  $\Phi := \Phi(\mathbf{I}_q - \mathbf{C}^+)^{\frac{1}{2}}$  and  $\mathbf{A}_s := (\mathbf{I}_q - \mathbf{C}^+)^{-\frac{1}{2}} \tilde{\mathbf{A}}_s$ . For any non-zero vector  $\mathbf{x}$ ,  $\mathbf{x}^T \mathbf{A}_s \mathbf{A}_s^T \mathbf{x} = 0$  implies that  $\mathbf{x}^T \mathbf{C}^+ \mathbf{x} = 0$ . Using similar arguments as in the preceding paragraph, we have  $\mathbb{C}(\mathbf{C}^+) \subseteq \bigcap_{s=1}^S \mathbb{C}(\mathbf{A}_s)$ .

Next we show that a non-null  $\bigcap_{s=1}^S \mathbb{C}(\mathbf{A}_s)$  guarantees the existence of a (not necessarily unique) psd matrix  $\mathbf{C}$  such that  $\mathbf{A}_s \mathbf{A}_s^T - \mathbf{C} \succeq \mathbf{0}$  for all  $s$  resulting in information switching. Let  $\mathbf{H} = [\mathbf{h}_1 \dots \mathbf{h}_r]$  be a  $q \times r$  matrix with orthonormal columns such that the columns form a basis of  $\bigcap_{s=1}^S \mathbb{C}(\mathbf{A}_s)$ . Let  $\mathbf{A}_s \mathbf{A}_s^T = \mathbf{H}_s \mathbf{D}_s \mathbf{H}_s^T$  be the spectral decomposition of  $\mathbf{A}_s \mathbf{A}_s^T$ . Clearly  $\mathbf{D}_s$  are diagonal matrices with non-negative entries. Let  $\varsigma$  be the minimum among all positive entries of  $\mathbf{D}_s$  across all  $s = 1, \dots, S$ . Define  $\mathbf{C} = \varsigma \mathbf{H} \mathbf{I}_r \mathbf{H}^T$ . By construction  $\mathbf{x}^T \mathbf{A}_s \mathbf{A}_s^T \mathbf{x} = 0$  implies that  $\mathbf{x}^T \mathbf{C} \mathbf{x} = 0$ . Also for  $\mathbf{x} \in \mathbb{C}(\mathbf{C})$ , we have  $0 < \mathbf{x}^T \mathbf{C} \mathbf{x} \leq \varsigma \|\mathbf{x}\|^2 \leq \mathbf{x}^T \mathbf{A}_s \mathbf{A}_s^T \mathbf{x}$ . Therefore,  $\mathbf{A}_s \mathbf{A}_s^T - \mathbf{C} \succeq \mathbf{0}$  for all  $s = 1, \dots, S$ , establishing the result.  $\square$

**Proof of Theorem 1.** when information switching occurs, Lemma 1 guarantees that  $\bigcap_{s=1}^S \mathbb{C}(\mathbf{A}_s)$  is non-null, so there exist vectors  $\mathbf{x}_1, \dots, \mathbf{x}_S$  such that  $\mathbf{A}_1 \mathbf{x}_1 = \dots = \mathbf{A}_S \mathbf{x}_S \neq \mathbf{0}$ . Now, for any non-degenerate continuous prior on  $\mathbf{A}_s, s = 1, \dots, S$ , the augmented matrix  $[\mathbf{A}_1 \dots \mathbf{A}_S]$  is full rank if and only if  $\sum_{s=1}^S q_s \leq q$ . Hence, the necessary and sufficient condition in Lemma 1 has zero prior support.  $\square$

**Proof of Theorem 2.** For two sequences  $a_n, b_n \geq 0$  we let  $a_n \asymp b_n$  imply  $0 < \liminf |a_n/b_n| \leq \limsup |a_n/b_n| < \infty$ . We define  $\Theta_n = \{\Lambda_n, \Delta_n, \mathbf{A}_{1n}, \dots, \mathbf{A}_{Sn}\}$  as the set of all parameters, and let  $\mathbb{P}_n$  and  $\mathbb{P}_{0n}$  denote the joint distributions of  $\mathcal{D}_n$  under  $\Theta_n$  and the true value  $\Theta_{0n}$ , respectively. to be the Kullback-Leibler (KL) divergence between  $\mathbb{P}_{0n}$  and  $\mathbb{P}_n$ .

Let  $\mathcal{P}_n = \mathcal{P}_{1,n} \cup \mathcal{P}_{2,n}$  be a partition of the parameter space  $\mathcal{P}_n$  where  $\mathcal{P}_{1,n} = \{\Theta_n : \|\mathbf{A}_{sn}\|_2^2 \leq Cn\tau_n^2 \text{ for all } s = 1, \dots, S\}$  for some large enough constant  $C > 0$  with  $n\tau_n^2 = c_n^2 q_{0n} s_n \log(d_n q_n)$  and  $\mathcal{P}_{2,n} = \mathcal{P}_{1,n}^c$ . Note that  $\Pi_n (\|\Sigma_n - \Sigma_{0n}\|_2 > M\varepsilon_n \mid \mathcal{D}_n) \leq \Pi_n (\Theta_n \in \mathcal{P}_{1,n} : \|\Sigma_n - \Sigma_{0n}\|_2 > M\varepsilon_n \mid \mathcal{D}_n) + \Pi_n (\mathcal{P}_{2,n} \mid \mathcal{D}_n)$ .

To prove the theorem, we show that, as  $n \rightarrow \infty$ , the posterior distribution on  $\mathcal{P}_{1,n}$  concentrates around  $\Sigma_{0n}$  while the remaining mass assigned to  $\mathcal{P}_{2,n}$  diminishes to zero. We define  $B_{n,0}(\Theta_{0n}, \epsilon) = \{\Theta_n \in \mathcal{P}_n : \mathbb{KL}(\mathbb{P}_{0n} \parallel \mathbb{P}_n) \leq n\epsilon^2\}$  as the set of probability measures characterized by  $\Theta_n$  within  $\epsilon$ -radius of  $\mathbb{P}_{0n}$  in KL divergence. We state the following lemma.

**Lemma 2.** *Let  $e_n$  be a semimetric on  $\mathcal{P}_n$  such that  $e_n(\Theta_n, \Theta_{0n}) = \frac{1}{n\tau_n^2 c_n^3} (\|\Sigma_n - \Sigma_{0n}\|_2 - c_n^2 \epsilon_n)$  where  $\epsilon_n \asymp c_n n \tau_n^3$ . Then  $\Pi_n \{\Theta_n \in \mathcal{P}_{1,n} : e_n(\Theta_n, \Theta_{0n}) > M\tau_n \mid \mathcal{D}_n\} \rightarrow 0$  in  $\mathbb{P}_{0n}$ -probability for a sufficiently large  $M$  as long as the following conditions hold for sufficiently large  $j \in \mathbb{N}$ :*

(I) *For some  $C > 0$ ,  $\Pi_n \{B_{n,0}(\Theta_{0n}, \tau_n)\} \geq e^{-Cn\tau_n^2}$ .*

(II) *Define the set  $G_{j,n} = \{\Theta_n \in \mathcal{P}_{1,n} : j\tau_n < e_n(\Theta_n, \Theta_{0n}) \leq 2j\tau_n\}$ . There exist test functions  $\varphi_n$  such that for some  $K > 0$ ,  $\lim_{n \rightarrow \infty} \mathbb{E}_{\Theta_{0n}} \varphi_n = 0$  and  $\sup_{\Theta_n \in G_{j,n}} \mathbb{E}_{\Theta_n} (1 - \varphi_n) \leq \exp(-Knj^2\tau_n^2)$ .*

The remaining technical arguments are included in full in the Supplemental Materials. We prove Lemma 2 in Section S.2.1, and verify condition (I) in Theorem 3 and show the existence of a sequence of test functions satisfying condition (II) in Theorem 4 there. Note that  $e_n(\Theta_n, \Theta_{0n}) > M\tau_n \Leftrightarrow \|\Sigma_n - \Sigma_{0n}\|_2 > M\epsilon_n$ . This implies that  $\Pi_n(\Theta_n \in \mathcal{P}_{1,n} : \|\Sigma_n - \Sigma_{0n}\|_2 > M\epsilon_n \mid \mathcal{D}_n) \rightarrow 0$  in  $\mathbb{P}_{0n}$ -probability. Subsequently applying the dominated convergence theorem (DCT) establishes that  $\lim_{n \rightarrow \infty} \mathbb{E}_{\mathbb{P}_{0n}} \Pi_n(\Theta_n \in \mathcal{P}_{1,n} : \|\Sigma_n - \Sigma_{0n}\|_2 > M\epsilon_n \mid \mathcal{D}_n) = 0$ . It remains to show that the remaining mass assigned to  $\mathcal{P}_{2,n}$  goes to 0, which is established in Theorem 5.  $\square$

**Proof of Corollary 1.** Let  $\mathbf{F}_{sn} = \Lambda_n \mathbf{A}_{sn} \mathbf{A}_{sn}^T \Lambda_n^T$  and  $\mathbf{F}_{0sn} = \Lambda_{0n} \mathbf{A}_{0sn} \mathbf{A}_{0sn}^T \Lambda_{0n}^T$ . Using the notations defined in the proof of Theorem 2, we have  $\Pi_n(\|\mathbf{F}_{sn} - \mathbf{F}_{0sn}\|_2 > M\epsilon_n \mid \mathcal{D}_n) \leq \Pi_n(\Theta_n \in \mathcal{P}_{1,n} : \|\mathbf{F}_{sn} - \mathbf{F}_{0sn}\|_2 > M\epsilon_n \mid \mathcal{D}_n) + \Pi_n(\mathcal{P}_{2,n} \mid \mathcal{D}_n)$ . As Theorem 5 in the supplementary materials shows that  $\Pi_n(\mathcal{P}_{2,n} \mid \mathcal{D}_n) \rightarrow 0$  in  $\mathbb{P}_{0n}$ -probability we focus on the first expression in the previous display in this proof.

Note that  $\Sigma_{0sn} = \Sigma_{0n} + \mathbf{F}_{0sn}$  and  $\Sigma_{sn} = \Sigma_n + \mathbf{F}_{sn}$ , and therefore  $\Pi_n(\Theta_n \in \mathcal{P}_{1,n} : \|\mathbf{F}_{sn} - \mathbf{F}_{0sn}\|_2 > M\epsilon_n \mid \mathcal{D}_n) \leq \Pi_n(\Theta_n \in \mathcal{P}_{1,n} : \|\Sigma_n - \Sigma_{0n}\|_2 > \frac{M}{2}\epsilon_n \mid \mathcal{D}_n) + \Pi_n(\Theta_n \in \mathcal{P}_{1,n} : \|\Sigma_{sn} - \Sigma_{0sn}\|_2 > \frac{M}{2}\epsilon_n \mid \mathcal{D}_n)$ . In Theorem 2 we established that the first term in the previous display diminishes to 0 in  $\mathbb{P}_{0n}$ -probability; in Theorem 6 of the supplementary materials we show that  $\Pi_n(\Theta_n \in \mathcal{P}_{1,n} : \|\Sigma_{sn} - \Sigma_{0sn}\|_2 > \frac{M}{2}\epsilon_n \mid \mathcal{D}_n) \rightarrow 0$  in  $\mathbb{P}_{0n}$ -probability. Hence  $\Pi_n(\|\mathbf{F}_{sn} - \mathbf{F}_{0sn}\|_2 > M\epsilon_n \mid \mathcal{D}_n) \rightarrow 0$  in  $\mathbb{P}_{0n}$ -probability. Subsequently applying DCT we conclude the proof.  $\square$

## A.2 Sampler Details and Distributed Computation

In this section, instead of  $\Delta$  we use its one-to-one transformation  $\tilde{\delta} = (\tilde{\delta}_1, \dots, \tilde{\delta}_d)^T = \log \text{diag}(\Delta)$ . It allows updating the  $\tilde{\delta}$  vector in the unrestricted space  $\mathbb{R}^d$  resulting in simplified numerical operations. Accordingly, we redefine  $\Theta := (\Lambda, \tilde{\delta}, \mathbf{A}_1, \dots, \mathbf{A}_S)$ .

**Gradients of the log-posterior:** Following Equation (8), we have

$$\log \Pi(\Theta | -) = \mathcal{L} + \log \Pi(\Lambda | \psi, \phi, \tau) + \log \Pi(\tilde{\delta}) + \sum_{s=1}^S \log \Pi(\mathbf{A}_s),$$

where  $\log \Pi(\Lambda | \psi, \phi, \tau) = K_\Lambda - \frac{1}{2\tau^2} \sum_{j=1}^d \sum_{h=1}^q \frac{\lambda_{j,h}^2}{\psi_{j,h} \phi_{j,h}^2}$ ,  $\log \Pi(\tilde{\delta}) = K_{\tilde{\delta}} - \frac{1}{2\sigma_{\tilde{\delta}}^2} \sum_{j=1}^d (\tilde{\delta}_j - \mu_{\tilde{\delta}})^2$  and  $\log \Pi(\mathbf{A}_s) = K_{\mathbf{A}_s} - \frac{1}{2b_{\mathbf{A}}} \sum_{j=1}^q \sum_{h=1}^{q_s} a_{s,j,h}^2$ . The constants  $K_\Lambda$ ,  $K_{\tilde{\delta}}$  and  $K_{\mathbf{A}_s}$ s are never required as they cancel out in the Metropolis-Hastings ratio. Analytical expressions for the partials of  $\log \Pi(\Lambda | -)$  are given below:

$$\frac{\partial}{\partial \Lambda} \log \Pi(\Theta | -) = - \sum_{s=1}^S \mathbf{G}_s \Lambda \mathbf{C}_s - \left( \frac{\lambda_{j,h}}{\psi_{j,h} \phi_{j,h}^2 \tau^2} \right)_{d \times q}, \quad (9)$$

$$\frac{\partial}{\partial \tilde{\delta}} \log \Pi(\Theta | -) = -\frac{1}{2} \sum_{s=1}^S \text{diag}(\mathbf{G}_s) \odot \exp(\tilde{\delta}) - \left( \frac{\tilde{\delta}_1 - \mu_{\tilde{\delta}}}{\sigma_{\tilde{\delta}}^2}, \dots, \frac{\tilde{\delta}_d - \mu_{\tilde{\delta}}}{\sigma_{\tilde{\delta}}^2} \right)^T, \quad (10)$$

$$\frac{\partial}{\partial \mathbf{A}_s} \log \Pi(\Theta | -) = -\Lambda^T \mathbf{G}_s \Lambda \mathbf{A}_s - \frac{1}{b_{\mathbf{A}}} \mathbf{A}_s, \quad (11)$$

where  $\mathbf{G}_s = n_s \Sigma_s^{-1} - \Sigma_s^{-1} \mathbf{W}_s \Sigma_s^{-1}$ ,  $\mathbf{C}_s = \mathbf{I}_q + \mathbf{A}_s \mathbf{A}_s^T$  and  $\odot$  denotes the Hadamard product between two vectors/matrices.

**Distributed gradient and likelihood computation:** In each HMC step of Algorithm 1, calculating  $\log \Pi(\Theta | -)$  and its gradients  $\frac{\partial}{\partial \Theta} \log \Pi(\Theta | -)$  are required for  $L$  many leapfrog operations. Note that the first terms in the RHS of (9)-(11) are gradients of  $\mathcal{L}$  with respect to parameters, while the second terms are gradients of the prior densities. Although computing the gradients of  $\mathcal{L}$  are seemingly intensive, these can be obtained very efficiently by dividing the calculations into parallel sub-operations across different studies. These sub-operations can be distributed over parallel processes in multi-thread computing systems. We elaborate the procedure in Algorithm 2, and illustrate it in a schematic diagram in Figure 5. The figure sketches out a flowchart to avoid repetitive calculations by storing variables and subsequently using them in following steps. The next lemma establishes its complexity.

**Lemma 3.** *The runtime complexity of each HMC step is  $\mathcal{O}(Lqd^2)$  with  $L$  being the number of leapfrog steps.*

*Proof.* Each HMC step comprises calculating the gradients of the log-posterior followed by evaluating the density at the proposed value. We separately compute the numerical complexities of each.

**Gradient computation:** As steps 7 and 8 are simply parallelized sums of objects with size at most  $qd$ , it suffices to focus attention on steps 2-5. These are parallelized

---

**Algorithm 2:** Distributed Gradient Computation of the log-likelihood  $\mathcal{L}$ 


---

```

1 parallel for  $s = 1, \dots, S$  do
2   Compute & store  $\mathbf{C}_s, \mathbf{C}_s^{1/2}, \tilde{\Lambda}_s = \mathbf{\Lambda} \mathbf{C}_s^{1/2}$  where  $\mathbf{C}_s^{1/2} = \text{Cholesky}(\mathbf{C}_s)$  and
       $\Sigma_s^{-1} = (\tilde{\Lambda}_s \tilde{\Lambda}_s^T + \Delta)^{-1} = \Delta^{-1} - \Delta^{-1} \tilde{\Lambda}_s (\mathbf{I}_q + \tilde{\Lambda}_s^T \Delta^{-1} \tilde{\Lambda}_s)^{-1} \tilde{\Lambda}_s^T \Delta^{-1}$ .
3   Compute & store  $\Sigma_s^{-1} \mathbf{W}_s$  and subsequently  $\mathbf{G}_s$ .
4   Compute & store  $\mathbf{G}_s \Delta$  and  $\mathbf{G}_s \Delta \mathbf{C}_s$ .
5   Compute  $\Delta^T \mathbf{G}_s \Delta \mathbf{A}_s$  to obtain  $\frac{\partial \mathcal{L}}{\partial \mathbf{A}_s}$ .
6 end
7 Sum the vectors  $\text{diag}(\mathbf{G}_s)$  from Step 3 across  $s = 1, \dots, S$  to obtain  $\frac{\partial \mathcal{L}}{\partial \delta}$ .
8 Sum the matrices  $\mathbf{G}_s \Delta \mathbf{C}_s$  from Step 4 across  $s = 1, \dots, S$  to obtain  $\frac{\partial \mathcal{L}}{\partial \Delta}$ .

```

---

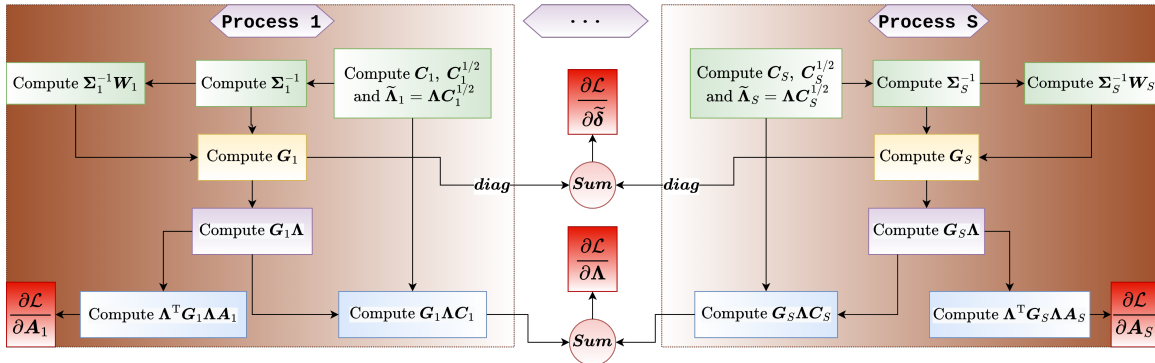


Figure 5: Schematic diagram of the distributed gradient computation.

across studies  $s = 1, \dots, S$ , so we analyze the cost for each study as follows.

**Step 2:** Computing the Cholesky factor  $\mathbf{C}_s^{1/2}$  is order  $\mathcal{O}(q^3)$  since  $\mathbf{C}_s$  has a low-rank plus diagonal decomposition, and Cholesky decomposition of a  $q \times q$  matrix is  $\mathcal{O}(q^3)$  in the worst case. Next, the matrix product  $\tilde{\Lambda}_s = \mathbf{\Lambda} \mathbf{C}_s^{1/2}$  is  $\mathcal{O}(q^2 d)$ . Finally, owing to the low-rank and diagonal decomposition structure, the inversion  $\Sigma_s^{-1}$  has complexity  $\mathcal{O}(q^2 d)$ . Therefore the overall complexity of this step is  $\mathcal{O}\{\max(q^2 d, q^3)\} = \mathcal{O}(q^2 d)$  since in our setting  $q \ll d$ .

**Step 3:** Noting that  $\Sigma_s^{-1} = (\tilde{\Lambda}_s \tilde{\Lambda}_s^T + \Delta)^{-1} = \Delta^{-1} - \Delta^{-1} \tilde{\Lambda}_s (\mathbf{I}_q + \tilde{\Lambda}_s^T \Delta^{-1} \tilde{\Lambda}_s)^{-1} \tilde{\Lambda}_s^T \Delta^{-1}$  reveals that computing  $\mathbf{G}_s$  is  $\mathcal{O}(qd^2)$ .

**Steps 4 and 5:** Because the factor  $\mathbf{G}_s$  is cached from the preceding step, obtaining the derivative (following the flowchart in Figure 5) only requires simple matrix multiplies, with complexity no more than  $\mathcal{O}(qd^2)$ .

Hence, the dominant complexity of steps 2-5 is  $\mathcal{O}(qd^2)$ , so that the combined computational complexity of all leapfrog steps is  $\mathcal{O}(Lqd^2)$ .

**log-posterior computation:** From equation (8) it can be seen that evaluating  $\mathcal{L}$  at a proposal is the expensive step involving high-dimensional matrix operations while the prior densities are quite simple to evaluate. Therefore, we focus on the complexity of calculating  $\mathcal{L}$ : owing to the structure of  $\Sigma_s$ ,  $|\Sigma_s|$  can be computed in  $\mathcal{O}(q^2d)$ . Using the already cached  $\Sigma_s^{-1}\mathbf{W}_s$  from step 3,  $\text{trace}(\Sigma_s^{-1}\mathbf{W}_s)$  can be computed in  $\mathcal{O}(d)$ . Both of the aforementioned operations are done in parallel across  $s$ , so evaluating the log-posterior has complexity no more than  $\mathcal{O}(q^2d)$ .

Hence, the runtime complexity of each HMC step is  $\mathcal{O}(Lqd^2)$ .  $\square$

## References

Amundsen, S. S. *et al.* (2010). Four novel coeliac disease regions replicated in an association study of a Swedish–Norwegian family cohort. *Genes & Immunity*, **11**, 79–86.

Armagan, A., Dunson, D. B., and Lee, J. (2013). Generalized double Pareto shrinkage. *Statistica Sinica*, **23**, 119–143.

Ashrafi, F., Ghezeldasht, S. A., and Ghobadi, M. Z. (2021). Identification of joint gene players implicated in the pathogenesis of HTLV-1 and BLV through a comprehensive system biology analysis. *Microbial Pathogenesis*, **160**, 105153.

Baglama, J. and Reichel, L. (2005). Augmented implicitly restarted Lanczos bidiagonalization methods. *SIAM Journal on Scientific Computing*, **27**, 19–42.

Bhattacharya, A. and Dunson, D. B. (2011). Sparse Bayesian infinite factor models. *Biometrika*, **98**, 291–306.

Bhattacharya, A., Pati, D., Pillai, N. S., and Dunson, D. B. (2015). Dirichlet-Laplace priors for optimal shrinkage. *Journal of the American Statistical Association*, **110**, 1479–1490.

Carvalho, C. M., Chang, J., Lucas, J. E., Nevins, J. R., Wang, Q., and West, M. (2008). High-dimensional sparse factor modeling: Applications in gene expression genomics. *Journal of the American Statistical Association*, **103**, 1438–1456.

Carvalho, C. M., Polson, N. G., and Scott, J. G. (2009). Handling sparsity via the horseshoe. In *Artificial Intelligence and Statistics*, pages 73–80. PMLR.

Chandra, N. K., Müller, P., and Sarkar, A. (2021). Bayesian precision factor analysis for high-dimensional sparse Gaussian graphical models. *arXiv:2107.11316*.

Chandra, N. K., Canale, A., and Dunson, D. B. (2023). Escaping the curse of dimensionality in Bayesian model-based clustering. *Journal of Machine Learning Research*. To appear.

Dai, F., Dutta, S., and Maitra, R. (2020). A matrix-free likelihood method for exploratory factor analysis of high-dimensional Gaussian data. *Journal of Computational and Graphical Statistics*, **29**, 675–680. PMID: 33041614.

De Vito, R., Bellio, R., Trippa, L., and Parmigiani, G. (2019). Multi-study factor analysis. *Biometrics*, **75**, 337–346.

De Vito, R., Bellio, R., Trippa, L., and Parmigiani, G. (2021). Bayesian multistudy factor analysis for high-throughput biological data. *The Annals of Applied Statistics*, **15**, 1723–1741.

Desch, A. N., Randolph, G. J., Murphy, K., *et al.* (2011). CD103+ pulmonary dendritic cells preferentially acquire and present apoptotic cell-associated antigen. *Journal of Experimental Medicine*, **208**, 1789–1797.

Elpek, K. G., Cremasco, V., Shen, H., *et al.* (2014). The tumor microenvironment shapes lineage, transcriptional, and functional diversity of infiltrating myeloid cells. *Cancer Immunology Research*, **2**, 655–667.

Erosheva, E. A. and Curtis, S. M. (2017). Dealing with reflection invariance in Bayesian factor analysis. *Psychometrika*, **82**, 295–307.

Fan, J., Fan, Y., and Lv, J. (2008). High dimensional covariance matrix estimation using a factor model. *Journal of Econometrics*, **147**, 186–197.

Franks, A. M. and Hoff, P. (2019). Shared subspace models for multi-group covariance estimation. *Journal of Machine Learning Research*, **20**, 1–37.

Frühwirth-Schnatter, S. and Lopes, H. F. (2018). Sparse Bayesian factor analysis when the number of factors is unknown. *arXiv preprint arXiv:1804.04231*.

Gelman, A. (2006). Prior distributions for variance parameters in hierarchical models. *Bayesian Analysis*, **1**, 515–534.

Gonzalez, H., Hagerling, C., and Werb, Z. (2018). Roles of the immune system in cancer: From tumor initiation to metastatic progression. *Genes & Development*, **32**, 1267–1284.

Green, P. J. (1995). Reversible jump Markov chain Monte Carlo computation and Bayesian model determination. *Biometrika*, **82**, 711–732.

Gu, Z., Gu, L., Eils, R., Schlesner, M., and Brors, B. (2014). *circlize* implements and enhances circular visualization in R. *Bioinformatics*, **30**, 2811–2812.

Hao, Q., Vadgama, J. V., and Wang, P. (2020). CCL2/CCR2 signaling in cancer pathogenesis. *Cell Communication and Signaling*, **18**, 1–13.

Heng, T. S., Painter, M. W., *et al.* (2008). The immunological genome project: networks of gene expression in immune cells. *Nature Immunology*, **9**, 1091–1094.

Iacob, E., Light, A. R., Donaldson, G. W., *et al.* (2016). Gene expression factor analysis to differentiate pathways linked to fibromyalgia, chronic fatigue syndrome, and depression in a diverse patient sample. *Arthritis Care & Research*, **68**, 132–140.

Ishwaran, H. and Rao, J. S. (2005). Spike and slab variable selection: Frequentist and Bayesian strategies. *The Annals of Statistics*, **33**, 730–773.

Kaiser, H. F. (1958). The varimax criterion for analytic rotation in factor analysis. *Psychometrika*, **23**, 187–200.

Kepler, T. B., Crosby, L., and Morgan, K. T. (2002). Normalization and analysis of DNA microarray data by self-consistency and local regression. *Genome Biology*, **3**, 1–12.

Knowles, D. and Ghahramani, Z. (2011). Nonparametric Bayesian sparse factor models with application to gene expression modeling. *The Annals of Applied Statistics*, **5**, 1534–1552.

Ksheera Sagar, K. N., Banerjee, S., Datta, J., and Bhadra, A. (2021). Precision matrix estimation under the horseshoe-like prior-penalty dual. arXiv:2104.10750.

Lee, P. Y., Wang, J.-X., Parisini, E., Dascher, C. C., and Nigrovic, P. A. (2013). Ly6 family proteins in neutrophil biology. *Journal of Leukocyte Biology*, **94**, 585–594.

Legramanti, S., Durante, D., and Dunson, D. B. (2020). Bayesian cumulative shrinkage for infinite factorizations. *Biometrika*, **107**, 745–752.

Levy, S. (2014). Function of the tetraspanin molecule CD81 in B and T cells. *Immunologic Research*, **58**, 179–185.

Liang, Y., Buckley, T. R., *et al.* (2001). Structural organization of the human MS4A gene cluster on chromosome 11q12. *Immunogenetics*, **53**, 357–368.

Limoges, M.-A., Cloutier, M., *et al.* (2021). The GIMAP family proteins: An incomplete puzzle. *Frontiers in Immunology*, **12**, 2046.

Lu, M.-J., Chen, C. Y.-H., and Härdle, W. K. (2017). Copula-based factor model for credit risk analysis. *Review of Quantitative Finance and Accounting*, **49**, 949–971.

Millsap, R. E. (2001). When trivial constraints are not trivial: The choice of uniqueness constraints in confirmatory factor analysis. *Structural Equation Modeling: A Multidisciplinary Journal*, **8**, 1–17.

Murray, J. S., Dunson, D. B., Carin, L., and Lucas, J. E. (2013). Bayesian Gaussian copula factor models for mixed data. *Journal of the American Statistical Association*, **108**, 656–665.

Neal, R. (2011). MCMC using Hamiltonian dynamics. In Chapter 5 of the Handbook of Markov Chain Monte Carlo Edited by Steve Brooks, Andrew Gelman, Galin Jones, and Xiao-Li Meng.

Painter, M. W., Davis, S., Hardy, R. R., *et al.* (2011). Transcriptomes of the B and T lineages compared by multiplatform microarray profiling. *The Journal of Immunology*, **186**, 3047–3057.

Papastamoulis, P. and Ntzoufras, I. (2022). On the identifiability of bayesian factor analytic models. *Statistics and Computing*, **32**, 23.

Parnet, P., Garka, K. E., *et al.* (1996). IL-1Rrp is a novel receptor-like molecule similar to the type I Interleukin-1 receptor and its homologues T1/ST2 and IL-1R AcP. *Journal of Biological Chemistry*, **271**, 3967–3970.

Pati, D., Bhattacharya, A., Pillai, N. S., and Dunson, D. (2014). Posterior contraction in sparse Bayesian factor models for massive covariance matrices. *The Annals of Statistics*, **42**, 1102–1130.

Poworoznek, E., Ferrari, F., and Dunson, D. (2021). Efficiently resolving rotational ambiguity in Bayesian matrix sampling with matching. *arXiv:2107.13783*.

Robert, C. P. and Roberts, G. (2021). Rao–Blackwellisation in the Markov chain Monte Carlo era. *International Statistical Review*, **89**, 237–249.

Ročková, V. and George, E. I. (2016). Fast Bayesian factor analysis via automatic rotations to sparsity. *Journal of the American Statistical Association*, **111**, 1608–1622.

Rohe, K. and Zeng, M. (2020). Vintage factor analysis with varimax performs statistical inference. *Journal of the Royal Statistical Society: Series B (Statistical Methodology)*. To appear.

Roy, A., Lavine, I., Herring, A. H., and Dunson, D. B. (2021). Perturbed factor analysis: Accounting for group differences in exposure profiles. *The Annals of Applied Statistics*, **15**, 1386–1404.

Russell, D. W. (2002). In search of underlying dimensions: The use (and abuse) of factor analysis in personality and social psychology bulletin. *Personality and Social Psychology Bulletin*, **28**(12), 1629–1646.

Sabnis, G., Pati, D., Engelhardt, B., and Pillai, N. (2016). A divide and conquer strategy for high dimensional Bayesian factor models. *arXiv:1612.02875*.

Sarkar, A., Pati, D., Mallick, B. K., and Carroll, R. J. (2021). Bayesian copula density deconvolution for zero-inflated data in nutritional epidemiology. *Journal of the American Statistical Association*, **116**, 1075–1087.

Schenk, R. L., Tuzlak, S., *et al.* (2017). Characterisation of mice lacking all functional isoforms of the pro-survival BCL-2 family member A1 reveals minor defects in the haematopoietic compartment. *Cell Death & Differentiation*, **24**, 534–545.

Schiavon, L., Canale, A., and Dunson, D. B. (2022). Generalized infinite factorization models. *Biometrika*, **109**, 817–835.

Tan, S., Li, D., and Zhu, X. (2020). Cancer immunotherapy: Pros, cons and beyond. *Biomedicine & Pharmacotherapy*, **124**, 109821.

Trendafilov, N. T., Fontanella, S., and Adachi, K. (2017). Sparse exploratory factor analysis. *Psychometrika*, **82**, 778–794.

Velasco-Velázquez, M., Jiao, X., *et al.* (2012). CCR5 antagonist blocks metastasis of basal breast cancer cells. *Cancer Research*, **72**, 3839–3850.

Wang, C., Gong, B., *et al.* (2014). The concordance between RNA-seq and microarray data depends on chemical treatment and transcript abundance. *Nature Biotechnology*, **32**, 926–932.

Watanabe, S. (2013). A widely applicable Bayesian information criterion. *Journal of Machine Learning Research*, **14**, 867–897.

Yoshida, H., Lareau, C. A., *et al.* (2019). The cis-regulatory atlas of the mouse immune system. *Cell*, **176**, 897–912.

Supplementary Materials for

# Inferring Covariance Structure from Multiple Data Sources via Subspace Factor Analysis

Noirrit Kiran Chandra<sup>†</sup>, David B. Dunson<sup>‡</sup>, Jason Xu<sup>‡,\*</sup>

<sup>†</sup>Department of Mathematical Sciences,  
The University of Texas at Dallas, Richardson, TX  
Email: noirrit.chandra@utdallas.edu

<sup>‡</sup>Department of Statistical Science, Duke University, Durham, NC

\*Department of Biostatistics and Bioinformatics, Duke University, Durham, NC

Supplementary materials provide further details on Hamiltonian Monte Carlo, complete prior specifications, proofs and details of the theoretical results and technical lemmas, extended simulation results, and details on the gene expression datasets.

## S.1 Details on Prior Specifications

**Specifics of the Dirichlet-Laplace (DL) prior:** On a  $d$ -dimensional vector  $\boldsymbol{\theta}$ , the DL prior with parameter  $a$ , denoted by  $\text{DL}(a)$ , can be specified hierarchically as

$$\theta_j \mid \boldsymbol{\psi}, \boldsymbol{\phi}, \tau \stackrel{\text{ind}}{\sim} N(0, \psi_j \phi_j^2 \tau^2), \quad \psi_j \stackrel{\text{iid}}{\sim} \text{Exp}\left(\frac{1}{2}\right), \quad \boldsymbol{\phi} \sim \text{Dir}(a, \dots, a), \quad \tau \sim \text{Ga}\left(da, \frac{1}{2}\right), \quad (\text{S.1})$$

where  $\theta_j$  is the  $j^{th}$  element of  $\boldsymbol{\theta}$ ,  $\tau \in \mathbb{R}$ ,  $\boldsymbol{\psi}, \boldsymbol{\phi} \in \mathbb{R}^d$ ,  $\text{Exp}(a)$  is an exponential distribution with mean  $1/a$ ,  $\text{Dir}(a_1, \dots, a_d)$  is the  $d$ -dimensional Dirichlet distribution, and  $\text{Ga}(a, b)$  is the gamma distribution with mean  $a/b$  and variance  $a/b^2$ .

**Choice of hyperparameters:** Following the suggestions by [Bhattacharya \*et al.\* \(2015\)](#) we set  $a = \frac{1}{2}$  as the DL hyperparameter. Recall that we have assumed  $a_{s,j,h} \stackrel{\text{iid}}{\sim} N(0, b_{\mathbf{A}})$  and  $\log \delta_j^2 \stackrel{\text{iid}}{\sim} N(\mu_{\delta}, \sigma_{\delta}^2)$  where  $\mathbf{A}_s = ((a_{s,j,h}))$  and  $\boldsymbol{\Delta} = \text{diag}(\delta_1^2, \dots, \delta_d^2)$ . To specify weakly informative priors, we set  $b_{\mathbf{A}} = 1$  and choose  $\mu_{\delta}, \sigma_{\delta}^2$  such that  $\mathbb{E}(\delta_j^2) = 1$  and  $\text{var}(\delta_j^2) = 10$  a priori for all  $j = 1, \dots, d$ .

## S.2 Proofs of Theoretical Results

**Notations:** For two sequences  $a_n, b_n \geq 0$ ,  $a_n \lesssim b_n$  implies that  $a_n \leq Cb_n$  for some constant  $C > 0$ ;  $a_n \asymp b_n$  implies that  $0 < \liminf |a_n/b_n| \leq \limsup |a_n/b_n| < \infty$ .  $|\mathbf{A}|$  denotes the determinant of the square matrix  $\mathbf{A}$ . For a set  $S$ ,  $|S|$  denotes its cardinality. Let  $\|\mathbf{x}\|$  be the Euclidean norm of a vector  $\mathbf{x}$ . We define  $\boldsymbol{\Theta}_n = \{\boldsymbol{\Lambda}_n, \boldsymbol{\Delta}_n, \mathbf{A}_{1n}, \dots, \mathbf{A}_{Sn}\}$  as the set of all parameters and  $\boldsymbol{\Theta}_{0n} = \{\boldsymbol{\Lambda}_{0n}, \boldsymbol{\Delta}_{0n}, \mathbf{A}_{01n}, \dots, \mathbf{A}_{0Sn}\}$  as the true data-generating values, and let  $\mathbb{P}_n$  and  $\mathbb{P}_{0n}$  denote the joint distributions of  $\mathcal{D}_n = \{\mathbf{Y}_{1,1}, \dots, \mathbf{Y}_{1,n_1}, \dots, \mathbf{Y}_{S,1}, \dots, \mathbf{Y}_{S,n_S}\}$  under  $\boldsymbol{\Theta}_n$  and the true value  $\boldsymbol{\Theta}_{0n}$ , respectively. We define  $\mathbb{KL}(\mathbb{P}_{0n} \parallel \mathbb{P}_n)$  to be the Kullback-Leibler (KL) divergence between  $\mathbb{P}_{0n}$  and  $\mathbb{P}_n$ .

For brevity of notations, we reuse  $C, \tilde{C}, C'',$  etc. in the proofs to denote constants whose values may not be the same throughout the same proof. Nevertheless, we are careful to make sure that these quantities are indeed constants.

We define the following quantities extensively used in the proofs

$$\tilde{\boldsymbol{\Lambda}}_{0n} = \begin{bmatrix} \boldsymbol{\Lambda}_{0n} & \mathbf{0}_{d_n \times (q_n - q_{0n})} \end{bmatrix} : \boldsymbol{\Lambda}_{0n} \text{ padded with } \mathbf{0} \text{ columns to have the same order as } \boldsymbol{\Lambda}_n,$$

$$\tilde{\mathbf{A}}_{0sn} = \begin{bmatrix} \mathbf{A}_{0sn} & \mathbf{0}_{q_{0sn} \times (q_{sn} - q_{0sn})} \end{bmatrix} : \mathbf{A}_{0sn} \text{ padded with } \mathbf{0} \text{ columns to have the same order as } \mathbf{A}_{sn},$$

$$\tilde{\boldsymbol{\Lambda}}_{0sn} = \tilde{\boldsymbol{\Lambda}}_{0n} \tilde{\mathbf{A}}_{0sn} : \text{product of the padded matrices to have the same order as } \boldsymbol{\Lambda}_n \mathbf{A}_{sn}.$$

**Theorem 3** (KL support).  $\Pi_n \{B_{n,0}(\mathbb{P}_{0n}, \tau_n)\} \geq e^{-Cn\tau_n^2}$  for  $n\tau_n^2 \asymp c_n^2 s_n q_{0n} \log(d_n q_n)$ .

*Proof.* Since the priors on  $\Lambda_n$ ,  $\mathbf{A}_{sn}$  and  $\Delta_n$  are independent, from Lemma 9, we have

$$\begin{aligned} \Pi_n \{B_{n,0}(\mathbb{P}_{0n}, \tau_n)\} &\geq \Pi_n \left\{ \sum_{s=1}^S \frac{n_s \|\Sigma_{0sn} - \Sigma_{sn}\|_F^2}{n \delta_{\min}^2(\Sigma_{sn})} \leq \tau_n^2 \right\} \\ &\geq \Pi_n \left( \left\| \Lambda_n - \tilde{\Lambda}_{0n} \right\|_F < \frac{C\tau_n}{q_{0n}\sqrt{c_n}} \right) \times \Pi_n \left( \max_{1 \leq s \leq S} \left\| \mathbf{A}_{sn} - \tilde{\mathbf{A}}_{0sn} \right\|_F < \frac{C\tau_n}{c_n\sqrt{q_{0n}}} \right) \\ &\quad \times \Pi_n \{ \|\Delta_{0n} - \Delta_n\|_F \leq C\tau_n, s_{\min}(\Delta_n) \geq \nu \}. \end{aligned} \quad (\text{S.2})$$

We handle the  $\mathbf{A}_s$ ,  $\Lambda$  and  $\Delta$  parts in (S.2) separately. We then conclude the proof by showing that each part individually exceeds  $e^{-Cn\tau_n^2}$  for some constant  $C > 0$ .

**The  $\mathbf{A}_{sn}$  term in (S.2):** Note that the priors on  $\mathbf{A}_{sn}$  are independent. Also from (C3)  $\left\| \tilde{\mathbf{A}}_{0sn} \right\|_F < \sqrt{q_{0sn}} \|\mathbf{A}_{0sn}\|_2 = o(\sqrt{q_{0sn}q_{0n}})$ . Further using Lemma 7 and the conditions  $\sum_{s=1}^S q_{0sn} \leq q_{0n}$  and  $\sum_{s=1}^S q_{sn} \leq q_n$ , we obtain

$$\begin{aligned} \Pi_n \left( \max_{1 \leq s \leq S} \left\| \mathbf{A}_{sn} - \tilde{\mathbf{A}}_{0sn} \right\|_F \leq \frac{C\tau_n}{c_n\sqrt{q_{0n}}} \right) &\geq e^{-C' \sum_{s=1}^S \max\{q_n q_{sn} \log \frac{c_n \sqrt{q_{0n}}}{\tau_n}, q_n q_{sn} \log(q_n q_{sn}), q_{0n} q_{0sn}\}} \\ &\geq e^{-C'' \max(q_n^2 \log \frac{c_n \sqrt{q_{0n}}}{\tau_n}, q_n^2 \log q_n, q_{0n}^2)}. \end{aligned} \quad (\text{S.3})$$

Using (D1) we get  $\max(q_n^2 \log q_n, q_{0n}^2) = o(n\tau_n^2)$ , and (D2) implies that  $q_n^2 \log \frac{c_n \sqrt{q_{0n}}}{\tau_n} = o\{c_n^2 s_n q_{0n} \log(d_n q_n)\}$ . Thus the quantity in (S.3) exceeds  $e^{-Cn\tau_n^2}$  for some  $C > 0$ .

**The  $\Lambda_n$  term in (S.2):** Using Pati *et al.* (2014, Lemma 7.1) we obtain

$$\Pi_n \left( \left\| \Lambda_n - \tilde{\Lambda}_{0n} \right\|_F < \frac{C\tau_n}{q_{0n}\sqrt{c_n}} \right) \geq e^{-C \max\left\{ \|\Lambda_{0n}\|_F^2, s_n q_{0n} \log \frac{s_n q_{0n}}{\frac{C\tau_n}{q_{0n}\sqrt{c_n}}}, \log(d_n q_n) \right\}}. \quad (\text{S.4})$$

Note that from (C3)  $\|\Lambda_{0n}\|_F^2 \leq q_{0n} \|\Lambda_{0n}\|_2^2 = o(c_n)$  and hence  $\max\{\|\Lambda_{0n}\|_F^2, \log(d_n q_n)\} = o(n\tau_n^2)$ . Additionally using (D2), we obtain that  $s_n q_{0n} \log \frac{s_n q_{0n}}{\frac{C\tau_n}{q_{0n}\sqrt{c_n}}} = \frac{1}{2} s_n q_{0n} \log \frac{n s_n q_{0n}^3}{c_n \log(d_n q_n)} = o\{c_n^2 s_n q_{0n} \log(d_n q_n)\}$ . Hence the RHS of (S.4) exceeds  $e^{-Cn\tau_n^2}$  for some  $C > 0$ .

**The  $\Delta_n$  term in (S.2):** Note that for a differentiable function  $f(\cdot)$  in a compact interval  $[a, b]$ , using the mean value theorem we have  $|f(w) - f(y)| = f'(x)(b - a)$  where  $a < w < x < y < b$  implying that  $|f(w) - f(y)| \leq (b - a) \times \sup_{x \in (a, b)} |f'(x)|$ . Thus we have  $\nu \leq \min_j \delta_{jn}^2 \leq \max_j \delta_{jn}^2 \leq c_n + M \Rightarrow |\delta_{jn}^2 - \delta_{0jn}^2| \leq (c_n + M) \log(c_n + M) |\log \delta_{jn}^2 - \log \delta_{0jn}^2| \leq C c_n \log c_n |\log \delta_{jn}^2 - \log \delta_{0jn}^2|$  where  $C, M > 0$  are positive large enough constants. Hence

$$\Pi_n \{ \|\Delta_n - \Delta_{0n}\|_F \leq C\tau_n, s_{\min}(\Delta_n) \geq \nu \}$$

$$\begin{aligned}
&\geq \Pi_n \left( \|\Delta_n - \Delta_{0n}\|_F \leq C\tau_n, \min_{1 \leq j \leq d_n} \delta_{jn}^2 \geq \nu, \max_{1 \leq j \leq d_n} \delta_{jn}^2 \leq c_n + M \right) \\
&\geq \Pi_n \left( \left\| \tilde{\delta}_n - \tilde{\delta}_{0n} \right\| \leq \frac{C'\tau_n}{c_n \log c_n}, \min_{1 \leq j \leq d_n} \delta_{jn}^2 \geq \nu, \max_{1 \leq j \leq d_n} \delta_{jn}^2 \leq c_n + M \right), \tag{S.5}
\end{aligned}$$

where  $\tilde{\delta}_n = (\log \delta_{1n}^2, \dots, \log \delta_{dn}^2)^T$  and  $\tilde{\delta}_{0n} = (\log \delta_{01n}^2, \dots, \log \delta_{0dn}^2)^T$ . Recall that  $\log \delta_{jn}^2 \stackrel{\text{iid}}{\sim} N(\mu_\delta, \sigma_\delta^2)$ . Adding a constant to the elements of  $\tilde{\delta}_{0n}$  does not violate any assumptions and therefore without loss of generality the parameter  $\mu_\delta$  can be assumed to be zero.

Note that  $\left\| \tilde{\delta}_n - \tilde{\delta}_{0n} \right\| \leq \frac{C'\tau_n}{c_n \log c_n} \Rightarrow \max_j |\log \delta_{jn}^2 - \log \delta_{0jn}^2| \leq \frac{C'\tau_n}{c_n \log c_n}$ . Since  $\tau_n = o(1)$  the last display in conjunction with (C4) further implies that  $\max_j \delta_{jn}^2 < \max_j \delta_{0jn}^2 + C''\tau_n < c_n + M$  and  $\min_j \delta_{jn}^2 > \min_j \delta_{0jn}^2 - C''\tau_n > \nu$ . Hence the set  $\left\{ \tilde{\delta}_n : \left\| \tilde{\delta}_n - \tilde{\delta}_{0n} \right\| \leq \frac{C'\tau_n}{c_n \log c_n} \right\}$  is a subset of  $\left\{ \min_{1 \leq j \leq d_n} \delta_{jn}^2 \geq \nu, \max_{1 \leq j \leq d_n} \delta_{jn}^2 \leq c_n + M \right\}$ . Therefore using Lemma 7

$$\begin{aligned}
\Pi_n \left\{ \|\Delta_n - \Delta_{0n}\|_F \leq C\tau_n, s_{\min}(\Delta_n) \geq \nu \right\} &\geq \Pi_n \left( \left\| \tilde{\delta}_n - \tilde{\delta}_{0n} \right\| \leq \frac{C'\tau_n}{c_n \log c_n} \right) \\
&\geq \exp \left\{ -C \max \left( d_n \log \frac{\sqrt{\sigma_\delta} c_n \log c_n}{\tau_n}, d_n \log d_n, \frac{1}{\sigma_\delta^2} \left\| \tilde{\delta}_{0n} \right\|^2 \right) \right\}. \tag{S.6}
\end{aligned}$$

Using (C3) we have  $\left\| \tilde{\delta}_{0n} \right\|^2 = o\{d_n(\log c_n)^2\}$ . Hence  $\max \left( d_n \log d_n, \frac{1}{\sigma_\delta^2} \left\| \tilde{\delta}_{0n} \right\|^2 \right) = o\{c_n^2 s_n q_{0n} \log(d_n q_n)\}$  using (C5). Additionally from (D2)  $d_n \frac{n\sigma_\delta(\log c_n)^2}{s_n q_{0n} \log(d_n q_n)} = o\{c_n^2 s_n q_{0n} \log(d_n q_n)\}$ . Thus the RHS of (S.6) exceeds  $e^{-Cn\tau_n^2}$  for some  $C > 0$ .

As we have shown that each of the product terms in (S.2) individually exceeds  $e^{-Cn\tau_n^2}$ , we conclude the proof.  $\square$

**Theorem 4** (Test function). *Recalling the definitions from the proof of Theorem 2, we let the set  $G_{j,n} = \{\Theta_n \in \mathcal{P}_{1,n} : j\tau_n \leq e_n(\Theta_n, \Theta_{0n}) \leq 2j\tau_n\}$  denote an annulus of inner and outer radii  $n\tau_n^2 c_n^3 (c_n^2 \epsilon_n + j\tau_n)$  and  $n\tau_n^2 c_n^3 (c_n^2 \epsilon_n + 2j\tau_n)$ , respectively, in spectral norm around  $\Sigma_{0n}$  for positive integer  $j = o\left[\frac{\sqrt{n}}{c_n^5} \{s_n q_{0n} \log(d_n q_n)\}^{-\frac{3}{2}}\right]$ . Based on observed data  $\mathcal{D}_n$  consider the following hypothesis testing problem  $H_0 : \Theta_n = \Theta_{0n}$  versus  $H_1 : \Theta_n \in G_{j,n}$ .*

Define  $\Lambda_{0sn} = \Lambda_{0n} \begin{bmatrix} \mathbf{I}_{q_{0n}} & \mathbf{A}_{0sn} \end{bmatrix}$ ,  $\tilde{q}_{0,sn} = q_{0n} + q_{0sn}$ ,  $\Delta_{\eta,0sn} = \Lambda_{0sn}^T \Delta_{0n}^{-1} \Lambda_{0sn}$ ,  $\Sigma_{\eta,0sn} = (\mathbf{I}_{\tilde{q}_{0,sn}} + \Delta_{\eta,0sn})^{-\frac{1}{2}}$ ,  $\Delta_{\eta,0sn} (\mathbf{I}_{\tilde{q}_{0,sn}} + \Delta_{\eta,0sn})^{-\frac{1}{2}}$  and  $\mathbf{Y}_{s,in} = (\mathbf{I}_{\tilde{q}_{0,sn}} + \Delta_{\eta,0sn})^{-1} \Lambda_{0sn}^T \Delta_{0n}^{-1} \mathbf{Y}_{s,i}$ . Further define  $\Xi_{sn} = \Sigma_{\eta,0sn}^{-\frac{1}{2}} (\sum_{i=1}^{n_s} \mathbf{Y}_{s,in} \mathbf{Y}_{s,in}^T) \Sigma_{\eta,0sn}^{-\frac{1}{2}}$  and the indicator functions  $\varphi_{sn} = \mathbb{1} \left( \left\| \frac{1}{n_s} \Xi_{sn} - \mathbf{I}_{\tilde{q}_{0,sn}} \right\|_2 > \epsilon_n \right)$  for  $s = 1, \dots, S$ . We define the test function:  $\varphi_n = 1 - \prod_{s=1}^S (1 - \varphi_{sn})$ . Then for some absolute constant  $K > 0$

$$\mathbb{E}_{H_0}(\varphi_n) \rightarrow 0; \quad \sup_{\Theta_n \in G_{j,n}} \mathbb{E}_{\Theta_n}(1 - \varphi_n) \leq \exp(-Knj^2\tau_n^2).$$

*Proof.* **Type-I error:** Note that under  $H_0$

$$\begin{aligned}
& \text{var}_{H_0}(\boldsymbol{\Upsilon}_{s,in}) \\
&= (\mathbf{I}_{\tilde{q}_{0,sn}} + \boldsymbol{\Delta}_{\eta,0sn})^{-1} \boldsymbol{\Lambda}_{0sn}^T \boldsymbol{\Delta}_{0n}^{-1} (\boldsymbol{\Lambda}_{0sn} \boldsymbol{\Lambda}_{0sn}^T + \boldsymbol{\Delta}_{0n}) \boldsymbol{\Delta}_{0n}^{-1} \boldsymbol{\Lambda}_{0sn} (\mathbf{I}_{\tilde{q}_{0,sn}} + \boldsymbol{\Delta}_{\eta,0sn})^{-1} \quad (\text{S.7}) \\
&= (\mathbf{I}_{\tilde{q}_{0,sn}} + \boldsymbol{\Delta}_{\eta,0sn})^{-1} (\boldsymbol{\Lambda}_{0sn}^T \boldsymbol{\Delta}_{0n}^{-1} \boldsymbol{\Lambda}_{0sn} \boldsymbol{\Lambda}_{0sn}^T \boldsymbol{\Delta}_{0n}^{-1} \boldsymbol{\Lambda}_{0sn} + \boldsymbol{\Lambda}_{0sn}^T \boldsymbol{\Delta}_{0n}^{-1} \boldsymbol{\Lambda}_{0sn}) (\mathbf{I}_{\tilde{q}_{0,sn}} + \boldsymbol{\Delta}_{\eta,0sn})^{-1} \\
&= (\mathbf{I}_{\tilde{q}_{0,sn}} + \boldsymbol{\Delta}_{\eta,0sn})^{-1} (\boldsymbol{\Delta}_{\eta,0sn}^2 + \boldsymbol{\Delta}_{\eta,0sn}) (\mathbf{I}_{\tilde{q}_{0,sn}} + \boldsymbol{\Delta}_{\eta,0sn})^{-1} \\
&= (\mathbf{I}_{\tilde{q}_{0,sn}} + \boldsymbol{\Delta}_{\eta,0sn})^{-\frac{1}{2}} \boldsymbol{\Delta}_{\eta,0sn} (\mathbf{I}_{\tilde{q}_{0,sn}} + \boldsymbol{\Delta}_{\eta,0sn})^{-\frac{1}{2}} = \boldsymbol{\Sigma}_{\eta,0sn},
\end{aligned}$$

implying that  $\boldsymbol{\Sigma}_{\eta,0sn}^{-\frac{1}{2}} \boldsymbol{\Upsilon}_{s,in} \stackrel{\text{iid}}{\sim} \mathcal{N}_q(\mathbf{0}, \mathbf{I}_{\tilde{q}_{0,sn}}) \Rightarrow \frac{1}{n_s} \mathbb{E}_{H_0}(\boldsymbol{\Xi}_{sn}) = \mathbf{I}_{\tilde{q}_{0,sn}}$  for all  $s = 1, \dots, S$ . From Vershynin (2012, Corollary 5.50),  $\mathbb{E}_{H_0}(\varphi_{sn}) \leq 2 \exp(-\tilde{C} \tilde{q}_{0,sn} t_n^2)$  for a universal constant  $\tilde{C} > 0$  and any sequence  $t_n$  satisfying  $\tilde{q}_{0,sn} t_n^2 \leq n_s \epsilon_n^2$ . From (C1), (C2) and (D1)  $\tilde{q}_{0,sn} \rightarrow \infty$  and  $n_s \epsilon_n^2 / \tilde{q}_{0,sn} > c_n^2 q_{0n} s_n \log(d_n q_n) \rightarrow \infty$  as  $n \rightarrow \infty$ . Hence  $t_n$  can be constructed such that  $t_n \succ 1$  and hence  $\lim_{n \rightarrow \infty} \mathbb{E}_{H_0}(\varphi_{sn}) = 0$ . Since the  $\varphi_{sn}$ s are independent across  $s$ ,  $\lim_{n \rightarrow \infty} \mathbb{E}_{H_0}(\varphi_n) = 1 - \prod_{s=1}^S \lim_{n \rightarrow \infty} \{1 - \mathbb{E}_{H_0}(\varphi_{sn})\} = 0$ .

**Type-II error:** For data generating parameters  $\boldsymbol{\Theta}_n \in G_{j,n}$ , we define  $\boldsymbol{\Sigma}_{\eta,sn} = \text{cov}(\boldsymbol{\Upsilon}_{s,in})$ . Then

$$\boldsymbol{\Sigma}_{\eta,sn} = (\mathbf{I}_{\tilde{q}_{0,sn}} + \boldsymbol{\Delta}_{\eta,0sn})^{-1} \boldsymbol{\Lambda}_{0sn}^T \boldsymbol{\Delta}_{0n}^{-1} (\boldsymbol{\Lambda}_{sn} \boldsymbol{\Lambda}_{sn}^T + \boldsymbol{\Delta}_n) \boldsymbol{\Delta}_{0n}^{-1} \boldsymbol{\Lambda}_{0sn} (\mathbf{I}_{\tilde{q}_{0,sn}} + \boldsymbol{\Delta}_{\eta,0sn})^{-1}.$$

Hence for  $\mathbf{z}_{s,i} \stackrel{\text{iid}}{\sim} \mathcal{N}_{\tilde{q}_{0,sn}}(\mathbf{0}, \mathbf{I}_{\tilde{q}_{0,sn}})$  for  $i = 1, \dots, n_s$ ,

$$\begin{aligned}
1 - \varphi_{sn} &= \mathbb{1} \left\{ \left\| \frac{1}{n_s} \boldsymbol{\Sigma}_{\eta,0sn}^{-\frac{1}{2}} \left( \sum_{i=1}^{n_s} \boldsymbol{\Upsilon}_{s,in} \boldsymbol{\Upsilon}_{s,in}^T \right) \boldsymbol{\Sigma}_{\eta,0sn}^{-\frac{1}{2}} - \mathbf{I}_{\tilde{q}_{0,sn}} \right\|_2 \leq \epsilon_n \right\} \\
&\leq \mathbb{1} \left\{ \left\| \frac{1}{n_s} \boldsymbol{\Sigma}_{\eta,0sn}^{-\frac{1}{2}} \left( \sum_{i=1}^{n_s} \boldsymbol{\Upsilon}_{s,in} \boldsymbol{\Upsilon}_{s,in}^T - \boldsymbol{\Sigma}_{\eta,sn} \right) \boldsymbol{\Sigma}_{\eta,0sn}^{-\frac{1}{2}} \right\|_2 \geq \left\| \boldsymbol{\Sigma}_{\eta,0sn}^{-\frac{1}{2}} \boldsymbol{\Sigma}_{\eta,sn} \boldsymbol{\Sigma}_{\eta,0sn}^{-\frac{1}{2}} - \mathbf{I}_{\tilde{q}_{0,sn}} \right\|_2 - \epsilon_n \right\} \\
&\leq \mathbb{1} \left( \left\| \boldsymbol{\Sigma}_{\eta,0sn}^{-1} \boldsymbol{\Sigma}_{\eta,sn} \right\|_2 \left\| \frac{1}{n_s} \sum_{i=1}^{n_s} \mathbf{z}_{s,i} \mathbf{z}_{s,i}^T - \mathbf{I}_{\tilde{q}_{0,sn}} \right\|_2 \geq \left\| \boldsymbol{\Sigma}_{\eta,0sn}^{-\frac{1}{2}} \boldsymbol{\Sigma}_{\eta,sn} \boldsymbol{\Sigma}_{\eta,0sn}^{-\frac{1}{2}} - \mathbf{I}_{\tilde{q}_{0,sn}} \right\|_2 - \epsilon_n \right). \quad (\text{S.8})
\end{aligned}$$

Note that,

$$\begin{aligned}
\boldsymbol{\Sigma}_{\eta,0sn}^{-\frac{1}{2}} \boldsymbol{\Sigma}_{\eta,sn} \boldsymbol{\Sigma}_{\eta,0sn}^{-\frac{1}{2}} - \mathbf{I}_{\tilde{q}_{0,sn}} &= \boldsymbol{\Sigma}_{\eta,0sn}^{-\frac{1}{2}} (\boldsymbol{\Sigma}_{\eta,sn} - \boldsymbol{\Sigma}_{\eta,0sn}) \boldsymbol{\Sigma}_{\eta,0sn}^{-\frac{1}{2}} \text{ and} \\
\boldsymbol{\Sigma}_{\eta,sn} - \boldsymbol{\Sigma}_{\eta,0sn} &= (\mathbf{I}_{\tilde{q}_{0,sn}} + \boldsymbol{\Delta}_{\eta,0sn})^{-1} \boldsymbol{\Lambda}_{0sn}^T \boldsymbol{\Delta}_{0n}^{-1} (\boldsymbol{\Sigma}_{sn} - \boldsymbol{\Sigma}_{0sn}) \boldsymbol{\Delta}_{0n}^{-1} \boldsymbol{\Lambda}_{0sn} (\mathbf{I}_{\tilde{q}_{0,sn}} + \boldsymbol{\Delta}_{\eta,0sn})^{-1} \\
\boldsymbol{\Sigma}_{\eta,0sn}^{-\frac{1}{2}} &= (\mathbf{I}_{\tilde{q}_{0,sn}} + \boldsymbol{\Delta}_{\eta,0sn})^{\frac{1}{2}} \left\{ \boldsymbol{\Lambda}_{0sn}^T \boldsymbol{\Delta}_{0n}^{-1} (\boldsymbol{\Lambda}_{0sn} \boldsymbol{\Lambda}_{0sn}^T + \boldsymbol{\Delta}_{0n}) \boldsymbol{\Delta}_{0n}^{-1} \boldsymbol{\Lambda}_{0sn} \right\}^{-\frac{1}{2}} (\mathbf{I}_{\tilde{q}_{0,sn}} + \boldsymbol{\Delta}_{\eta,0sn})^{\frac{1}{2}}.
\end{aligned}$$

We obtain the last identity in the above display from (S.7). Therefore,

$$\begin{aligned} \Sigma_{\eta,0sn}^{-\frac{1}{2}} \Sigma_{\eta,sn} \Sigma_{\eta,0sn}^{-\frac{1}{2}} - \mathbf{I}_{\tilde{q}_{0,sn}} &= (\mathbf{I}_{\tilde{q}_{0,sn}} + \Delta_{\eta,0sn})^{\frac{1}{2}} \{ \Lambda_{0sn}^T \Delta_{0n}^{-1} (\Lambda_{0sn} \Lambda_{0sn}^T + \Delta_{0n}) \Delta_{0n}^{-1} \Lambda_{0sn} \}^{-\frac{1}{2}} \\ &\quad \times (\mathbf{I}_{\tilde{q}_{0,sn}} + \Delta_{\eta,0sn})^{-\frac{1}{2}} \Lambda_{0sn}^T \Delta_{0n}^{-1} (\Sigma_{sn} - \Sigma_{0sn}) \Delta_{0n}^{-1} \Lambda_{0sn} (\mathbf{I}_{\tilde{q}_{0,sn}} + \Delta_{\eta,0sn})^{-\frac{1}{2}} \\ &\quad \times \{ \Lambda_{0sn}^T \Delta_{0n}^{-1} (\Lambda_{0sn} \Lambda_{0sn}^T + \Delta_{0n}) \Delta_{0n}^{-1} \Lambda_{0sn} \}^{-\frac{1}{2}} (\mathbf{I}_{\tilde{q}_{0,sn}} + \Delta_{\eta,0sn})^{\frac{1}{2}}. \end{aligned}$$

Lemma 6 implies that

$$\begin{aligned} \left\| \Sigma_{\eta,0sn}^{-\frac{1}{2}} \Sigma_{\eta,sn} \Sigma_{\eta,0sn}^{-\frac{1}{2}} - \mathbf{I}_{\tilde{q}_{0,sn}} \right\|_2 &\geq \|\Sigma_{sn} - \Sigma_{0sn}\|_2 \times s_{\min}^2 \left[ (\mathbf{I}_{\tilde{q}_{0,sn}} + \Delta_{\eta,0sn})^{\frac{1}{2}} \times \right. \\ &\quad \left. \{ \Lambda_{0sn}^T \Delta_{0n}^{-1} (\Lambda_{0sn} \Lambda_{0sn}^T + \Delta_{0n}) \Delta_{0n}^{-1} \Lambda_{0sn} \}^{-\frac{1}{2}} \times (\mathbf{I}_{\tilde{q}_{0,sn}} + \Delta_{\eta,0sn})^{-\frac{1}{2}} \Lambda_{0sn}^T \Delta_{0n}^{-1} \right]. \quad (\text{S.9}) \end{aligned}$$

Let us define  $\boldsymbol{\chi}_{0sn} = \Delta_{0n}^{-\frac{1}{2}} \Lambda_{0sn}$ . Then  $\Delta_{\eta,0sn} = \boldsymbol{\chi}_{0sn}^T \boldsymbol{\chi}_{0sn}$  and the term inside the  $s_{\min}^2$  in (S.9) simplifies to

$$\begin{aligned} (\mathbf{I}_{\tilde{q}_{0,sn}} + \boldsymbol{\chi}_{0sn}^T \boldsymbol{\chi}_{0sn})^{\frac{1}{2}} \times \{ \boldsymbol{\chi}_{0sn}^T (\boldsymbol{\chi}_{0sn} \boldsymbol{\chi}_{0sn}^T + \mathbf{I}_{d_n}) \boldsymbol{\chi}_{0sn} \}^{-\frac{1}{2}} \\ \times (\mathbf{I}_{\tilde{q}_{0,sn}} + \boldsymbol{\chi}_{0sn}^T \boldsymbol{\chi}_{0sn})^{-\frac{1}{2}} \boldsymbol{\chi}_{0sn}^T \Delta_{0n}^{-\frac{1}{2}}. \quad (\text{S.10}) \end{aligned}$$

Letting  $\chi_{0s,rn}$ ,  $r = 1, \dots, \tilde{q}_{0,sn}$  denote the eigenvalues of  $\boldsymbol{\chi}_{0sn}^T \boldsymbol{\chi}_{0sn}$  and using Lemma 6, we have

$$\begin{aligned} s_{\min}^2 \left[ (\mathbf{I}_{\tilde{q}_{0,sn}} + \boldsymbol{\chi}_{0sn}^T \boldsymbol{\chi}_{0sn})^{\frac{1}{2}} \times \{ \boldsymbol{\chi}_{0sn}^T (\boldsymbol{\chi}_{0sn} \boldsymbol{\chi}_{0sn}^T + \mathbf{I}_{d_n}) \boldsymbol{\chi}_{0sn} \}^{-\frac{1}{2}} \right. \\ \left. \times (\mathbf{I}_{\tilde{q}_{0,sn}} + \boldsymbol{\chi}_{0sn}^T \boldsymbol{\chi}_{0sn})^{-\frac{1}{2}} \boldsymbol{\chi}_{0sn}^T \Delta_{0n}^{-\frac{1}{2}} \right] &\geq s_{\min} (\Delta_{0n}^{-1}) \times \\ \left[ \min_{r=1, \dots, \tilde{q}_{0,sn}} \left\{ (1 + \chi_{0s,rn})^{\frac{1}{2}} (\chi_{0s,rn} (1 + \chi_{0s,rn}))^{-\frac{1}{2}} (1 + \chi_{0s,rn})^{-\frac{1}{2}} \chi_{0s,rn}^{\frac{1}{2}} \right\} \right]^2 \\ &\geq \frac{1}{\|\Delta_{0n}\|_2} \times \min_{r=1, \dots, \tilde{q}_{0,sn}} \frac{1}{1 + \chi_{0s,rn}} \geq \frac{1}{\|\Delta_{0n}\|_2} \times \frac{1}{1 + \|\Lambda_{0sn}^T \Delta_{0n}^{-1} \Lambda_{0sn}\|_2}. \quad (\text{S.11}) \end{aligned}$$

From (C3)-(C4)  $\|\Delta_{0n}\|_2 = o(c_n)$ ,  $\|\Lambda_{0sn}\|_2^2 = o(c_n)$ . Now combining (S.9)-(S.11), we get

$$\begin{aligned} \left\| \Sigma_{\eta,0sn}^{-\frac{1}{2}} \Sigma_{\eta,sn} \Sigma_{\eta,0sn}^{-\frac{1}{2}} - \mathbf{I}_{\tilde{q}_{0,sn}} \right\|_2 &\geq \frac{\|\Sigma_{sn} - \Sigma_{0sn}\|_2}{\|\Delta_{0n}\|_2 (1 + \|\Lambda_{0sn}^T \Delta_{0n}^{-1} \Lambda_{0sn}\|_2)} \\ &\geq \frac{\|\Sigma_{sn} - \Sigma_{0n}\|_2}{\|\Delta_{0n}\|_2 \left( 1 + \frac{\|\Lambda_{0sn}\|_2^2}{\delta_{\min}^2} \right)} \geq \frac{\|\Sigma_{sn} - \Sigma_{0n}\|_2}{c_n^2}. \quad (\text{S.12}) \end{aligned}$$

Similarly, we have

$$\begin{aligned} \|\Sigma_{\eta,0sn}^{-1} \Sigma_{\eta,sn}\|_2 &\leq \|\Sigma_{sn}\|_2 \times \left\| (\mathbf{I}_{\tilde{q}_{0,sn}} + \Delta_{\eta,0sn})^{\frac{1}{2}} \times \right. \\ &\quad \left. \left\{ \Lambda_{0sn}^T \Delta_{0n}^{-\frac{1}{2}} (\Lambda_{0sn} \Lambda_{0sn} + \Delta_{0n}) \Delta_{0n}^{-\frac{1}{2}} \Lambda_{0sn} \right\}^{-\frac{1}{2}} \times (\mathbf{I}_{\tilde{q}_{0,sn}} + \Delta_{\eta,0sn})^{-\frac{1}{2}} \Lambda_{0sn}^T \Delta_{0n}^{-1} \right\|_2^2 \\ &\leq \|\Sigma_{sn}\|_2 \times \left[ \max_{1 \leq r \leq \tilde{q}_{0,sn}} \left\{ (1 + \chi_{0s,rn})^{\frac{1}{2}} (\chi_{0s,rn}(1 + \chi_{0s,rn}))^{-\frac{1}{2}} (1 + \chi_{0s,rn})^{-\frac{1}{2}} \chi_{0s,rn}^{\frac{1}{2}} \right\} \right]^2 \quad (\text{S.13}) \end{aligned}$$

$$\leq \|\Sigma_n\|_2 + \|\Lambda_n \mathbf{A}_{sn} \mathbf{A}_{sn}^T \Lambda_n^T\|_2 \leq \|\Sigma_n\|_2 (1 + \|\mathbf{A}_{sn}\|_2^2). \quad (\text{S.14})$$

Note that  $\|\Sigma_n\|_2 \leq \|\Sigma_n - \Sigma_{0n}\|_2 + c_n$ . Combining (S.8), (S.12) and (S.14) we get

$$\begin{aligned} 1 - \varphi_{sn} &\leq \mathbb{1} \left\{ \|\Sigma_n\|_2 (1 + \|\mathbf{A}_{sn}\|_2^2) \left\| \frac{1}{n_s} \sum_{i=1}^{n_s} \mathbf{z}_{s,i} \mathbf{z}_{s,i}^T - \mathbf{I}_{\tilde{q}_{0,sn}} \right\|_2 \geq \frac{\|\Sigma_n - \Sigma_{0n}\|_2}{c_n^2} - \epsilon_n \right\} \\ &\leq \mathbb{1} \left\{ \left\| \frac{1}{n_s} \sum_{i=1}^{n_s} \mathbf{z}_{s,i} \mathbf{z}_{s,i}^T - \mathbf{I}_{\tilde{q}_{0,sn}} \right\|_2 \geq \frac{\|\Sigma_n - \Sigma_{0n}\|_2 - \epsilon_n c_n^2}{c_n^2 (\|\Sigma_n - \Sigma_{0n}\|_2 + c_n) (1 + \|\mathbf{A}_{sn}\|_2^2)} \right\}, \quad (\text{S.15}) \end{aligned}$$

where  $\mathbf{z}_{s,1:n_s} \stackrel{\text{iid}}{\sim} \mathcal{N}_{\tilde{q}_{0,sn}}(\mathbf{0}, \mathbf{I}_{\tilde{q}_{0,sn}})$ . Using Lemma 10, we see that the RHS of (S.15) is bounded below by  $(\tilde{C} \sqrt{\tilde{q}_{0,sn}} + j \sqrt{n} \tau_n) \frac{1}{\sqrt{n_s}}$  for some absolute constant  $\tilde{C} > 0$  if  $\Theta_n \in G_{j,n}$ . Further applying Vershynin (2012, Equation 5.26), for all  $\Theta_n \in G_{j,n}$  we get

$$\mathbb{E}_{\Theta_n} (1 - \varphi_{sn}) \leq \Pr \left\{ \left\| \frac{1}{n_s} \sum_{i=1}^{n_s} \mathbf{z}_{s,i} \mathbf{z}_{s,i}^T - \mathbf{I}_{\tilde{q}_{0,sn}} \right\|_2 \geq (\tilde{C} \sqrt{\tilde{q}_{0,sn}} + j \sqrt{n} \tau_n) \frac{1}{\sqrt{n_s}} \right\} \leq e^{-K j^2 n_s \tau_n^2}.$$

Finally,  $\sup_{\Theta_n \in G_{j,n}} \mathbb{E}_{\Theta_n} (1 - \varphi_n) = \sup_{\Theta_n \in G_{j,n}} \prod_{s=1}^S \mathbb{E}_{\Theta_n} (1 - \varphi_{sn}) \leq e^{-K (\sum_{s=1}^S n_s) j^2 \tau_n^2}$ .  
Hence the proof.  $\square$

**Theorem 5** (Remaining probability mass).  $\lim_{n \rightarrow \infty} \mathbb{E}_{\mathbb{P}_{0n}} \Pi_n (\mathcal{P}_{2,n} \mid \mathcal{D}_n) = 0$ .

*Proof.* For densities  $\mathbf{p}_{0n}$  and  $\mathbf{p}_n$  corresponding to  $\mathbb{P}_{0n}$  and  $\mathbb{P}_n$ , respectively, we define the average KL variation  $\mathbb{V}(\mathbb{P}_{0n} \parallel \mathbb{P}_n) = \int \left\{ \log \frac{\mathbf{p}_{0n}}{\mathbf{p}_n} - \mathbb{KL}(\mathbb{P}_{0n} \parallel \mathbb{P}_n) \right\}^2 d\mathbf{p}_{0n}$  and the set  $B_{n,2}(\mathbb{P}_{0n}, \tau) = \{\mathbb{P}_n : \mathbb{KL}(\mathbb{P}_{0n} \parallel \mathbb{P}_n) \leq n\tau^2, \mathbb{V}(\mathbb{P}_{0n} \parallel \mathbb{P}_n) \leq n\tau^2\}$ .

From Banerjee and Ghosal (2015, Theorem 3.1) we find that the KL variation between  $\mathcal{N}_{d_n}(\mathbf{0}, \Sigma_{0sn})$  and  $\mathcal{N}_{d_n}(\mathbf{0}, \Sigma_{sn})$  is  $\frac{1}{2} \sum_{j=1}^{d_n} (1 - \psi_j)^2$  where  $\psi_j$ 's are eigenvalues of  $\Sigma_{sn}^{-\frac{1}{2}} \Sigma_{0sn} \Sigma_{sn}^{-\frac{1}{2}}$ . Hence  $\mathbb{V}(\mathbb{P}_{0n} \parallel \mathbb{P}_n) = \sum_{s=1}^S n_s \|\Sigma_{sn}^{-1} (\Sigma_{0sn} - \Sigma_{sn})^2 \Sigma_{sn}^{-1}\|_F^2 \leq \sum_{s=1}^S \frac{n_s \|\Sigma_{0sn} - \Sigma_{sn}\|_F^2}{2s_{\min}^2(\Sigma_{sn})}$ . Therefore, the same three conditions in Lemma 9 imply that  $2\mathbb{V}(\mathbb{P}_{0n} \parallel \mathbb{P}_n) \leq n\tau_n^2$  and accordingly  $\Pi_n \{B_{n,2}(\mathbb{P}_{0n}, \tau_n)\} > e^{-\tilde{C} n \tau_n^2}$  for some absolute constant  $\tilde{C} > 0$ .

Note that the elements of  $\mathbf{A}_{sn}$  are iid  $N(0, b_{\mathbf{A}})$  across all  $s$ . Thus using [Vershynin \(2012, Theorem 5.39\)](#) we get that  $\Pi_n(\|\mathbf{A}_{sn}\|_2 \geq C\sqrt{n\tau_n^2}) \leq e^{-C'n\tau_n^2}$  with  $C'$  depending only on the constants  $b_{\mathbf{A}}$  and  $C$ . Therefore  $\Pi_n(\mathcal{P}_{2,n}) \leq \sum_{s=1}^S \Pi_n(\|\mathbf{A}_{sn}\|_2 \geq C\sqrt{n\tau_n^2}) \leq e^{-C''n\tau_n^2}$  where  $C''$  is a constant that depends only on the constants  $b_{\mathbf{A}}$ ,  $S$  and  $C$ . Hence,  $\frac{\Pi_n(\mathcal{P}_{2,n})}{\Pi_n\{B_{n,2}(\mathbb{P}_{0n}, \tau_n)\}} \leq e^{-2(C'' - \tilde{C})n\tau_n^2} = o(e^{-2n\tau_n^2})$ . The last display holds if the constant  $C$  in the definition of  $\mathcal{P}_{2,n}$  is large enough, however, it is independent of  $n$ . Using [Ghosal and van der Vaart \(2017, Theorem 8.20\)](#) and subsequent application of DCT we conclude the proof.  $\square$

**Theorem 6.** *Under the same conditions of Theorem 2,  $\Pi_n(\Theta_n \in \mathcal{P}_{1,n} : \|\Sigma_{sn} - \Sigma_{0sn}\|_2 > M\varepsilon_n \mid \mathcal{D}_n) \rightarrow 0$  in  $\mathbb{P}_{0n}$ -probability.*

*Proof.* Recall  $\epsilon_n \asymp c_n n\tau_n^3$  and  $n\tau_n^2 = c_n^2 s_n q_{0n} \log(d_n q_n)$  defined in the proof of Theorem 2. Using these we now state a variation of Lemma 2. stated earlier.

**Lemma 4.** *Let  $\tilde{e}_n^{(s)}$  be a semimetric on  $\mathcal{P}_n$  such that  $\tilde{e}_n^{(s)}(\Theta_n, \Theta_{0n}) = \frac{1}{c_n^3}(\|\Sigma_{sn} - \Sigma_{0sn}\|_2 - c_n^2 \epsilon_n - \frac{c_n^3 \tilde{q}_{0,sn}}{\sqrt{n_s}})$ . Then  $\Pi_n\left\{\Theta_n \in \mathcal{P}_{1,n} : \tilde{e}_n^{(s)}(\Theta_n, \Theta_{0n}) > C\tau_n \mid \mathcal{D}_n\right\} \rightarrow 0$  in  $\mathbb{P}_{0n}$ -probability for a sufficiently large  $M$  and a constant  $C > 0$ , if for every sufficiently large  $j \in \mathbb{N}$  the following conditions hold*

(I') *For some  $C > 0$ ,  $\Pi_n\{B_{n,0}(\Theta_{0n}, \tau_n)\} \geq e^{-Cn\tau_n^2}$ .*

(II') *Define the set  $\tilde{G}_{j,n} = \left\{\Theta_n \in \mathcal{P}_{1,n} : j\tau_n < \tilde{e}_n^{(s)}(\Theta_n, \Theta_{0n}) \leq 2j\tau_n\right\}$ . There exists tests  $\varphi_{sn}$  such that for some  $K > 0$ ,  $\lim_{n \rightarrow \infty} \mathbb{E}_{\Theta_{0n}} \varphi_{sn} = 0$  and  $\sup_{\Theta_n \in \tilde{G}_{j,n}} \mathbb{E}_{\Theta_n} (1 - \varphi_{sn}) \leq \exp(-Knj^2\tau_n^2)$ .*

Proof of the above lemma follows same line of arguments as Lemma 2. Additionally condition (I') is identical to (I) from Lemma 2. We show the existence of a sequence of test functions satisfying condition (II') in Lemma 5. This implies that

$$\Pi_n\{\Theta_n \in \mathcal{P}_{1,n} : \tilde{e}_n^{(s)}(\Theta_n, \Theta_{0n}) > C\tau_n \mid \mathcal{D}_n\} \rightarrow 0 \text{ in } \mathbb{P}_{0n}\text{-probability.} \quad (\text{S.16})$$

Note that  $\tilde{e}_n^{(s)}(\Theta_n, \Theta_{0n}) > C\tau_n \Leftrightarrow \|\Sigma_{sn} - \Sigma_{0sn}\|_2 > c_n^2 \epsilon_n + \frac{c_n^3 \tilde{q}_{0,sn}}{\sqrt{n_s}} + Cc_n^3 \tau_n$ . From respective definitions of  $\epsilon_n$  and  $\varepsilon_n$ ,  $c_n^2 \epsilon_n \asymp \varepsilon_n$  and from (D1)  $\varepsilon_n \succ \max\left(\frac{c_n^3 \tilde{q}_{0,sn}}{\sqrt{n_s}}, c_n^3 \tau_n\right)$ . Thus (S.16) implies that for some large enough  $M$ ,  $\Pi_n(\Theta_n \in \mathcal{P}_{1,n} : \|\Sigma_{sn} - \Sigma_{0sn}\|_2 > M\varepsilon_n \mid \mathcal{D}_n) \rightarrow 0$  in  $\mathbb{P}_{0n}$ -probability.  $\square$

**Lemma 5.** *Recalling the definitions from Lemma 4, we let the set  $\tilde{G}_{j,n} = \{\Theta_n \in \mathcal{P}_{1,n} : j\tau_n \leq \tilde{e}_n^{(s)}(\Theta_n, \Theta_{0n}) \leq 2j\tau_n\}$  for positive integer  $j = o\left[\sqrt{n}\{c_n^2 s_n q_{0n} \log(d_n q_n)\}^{-\frac{1}{2}}\right]$ . Based on observed data  $\mathcal{D}_n$  consider the following hypothesis testing problem  $H_0 : \Theta_n = \Theta_{0n}$  versus  $H_1 : \Theta_n \in \tilde{G}_{j,n}$ . We use  $\varphi_{sn} = \mathbb{1}\left(\left\|\frac{1}{n_s} \mathbf{\Xi}_{sn} - \mathbf{I}_{\tilde{q}_{0,sn}}\right\|_2 > \epsilon_n\right)$  from Theorem 4 as the test function. Then for some absolute constant  $K > 0$*

$$\mathbb{E}_{H_0}(\varphi_{sn}) \rightarrow 0; \quad \sup_{\Theta_n \in \tilde{G}_{j,n}} \mathbb{E}_{\Theta_n} (1 - \varphi_{sn}) \leq \exp(-Knj^2\tau_n^2).$$

*Proof. Type-I error:* Please refer to corresponding section in the proof of Theorem 4 where it has already been established that  $\lim_{n \rightarrow \infty} \mathbb{E}_{H_0}(\varphi_{sn}) = 0$ .

**Type-II error:** From eqn (S.13),

$$\|\Sigma_{\eta,0sn}^{-1} \Sigma_{\eta,sn}\|_2 \leq \|\Sigma_{sn}\|_2 \leq \|\Sigma_{sn} - \Sigma_{0sn}\|_2 + \|\Sigma_{sn}\|_2 < \|\Sigma_{sn} - \Sigma_{0sn}\|_2 + c_n. \quad (\text{S.17})$$

We obtain the last inequality in the previous display using (C3) and (C4). Using (S.12)

$$\left\| \Sigma_{\eta,0sn}^{-\frac{1}{2}} \Sigma_{\eta,sn} \Sigma_{\eta,0sn}^{-\frac{1}{2}} - \mathbf{I}_{\tilde{q}_{0,sn}} \right\|_2 \geq \frac{\|\Sigma_{sn} - \Sigma_{0sn}\|_2}{\|\Delta_{0n}\|_2 (1 + \|\Lambda_{0sn}^T \Delta_{0n}^{-1} \Lambda_{0sn}\|_2)} \geq \frac{\|\Sigma_{sn} - \Sigma_{0sn}\|_2}{c_n^2}. \quad (\text{S.18})$$

Combining (S.8), (S.17) and (S.18) we get

$$\begin{aligned} & 1 - \varphi_{sn} \\ & \leq \mathbb{1} \left\{ (\|\Sigma_{sn} - \Sigma_{0sn}\|_2 + c_n) \left\| \frac{1}{n_s} \sum_{i=1}^{n_s} \mathbf{z}_{s,i} \mathbf{z}_{s,i}^T - \mathbf{I}_{\tilde{q}_{0,sn}} \right\|_2 \geq \frac{\|\Sigma_{sn} - \Sigma_{0sn}\|_2}{c_n^2} - \epsilon_n \right\} \\ & \leq \mathbb{1} \left\{ \left\| \frac{1}{n_s} \sum_{i=1}^{n_s} \mathbf{z}_{s,i} \mathbf{z}_{s,i}^T - \mathbf{I}_{\tilde{q}_{0,sn}} \right\|_2 \geq \frac{\|\Sigma_{sn} - \Sigma_{0sn}\|_2 - \epsilon_n c_n^2}{c_n^2 (\|\Sigma_{sn} - \Sigma_{0sn}\|_2 + c_n)} \right\}. \end{aligned} \quad (\text{S.19})$$

Using  $j = o \left[ \sqrt{n} \{c_n^2 s_n q_{0n} \log(d_n q_n)\}^{-\frac{1}{2}} \right]$  and similar arguments as in the proof of Lemma 10, it can be straightforwardly seen that  $\frac{\|\Sigma_{sn} - \Sigma_{0sn}\|_2 - \epsilon_n c_n^2}{c_n^2 (\|\Sigma_{sn} - \Sigma_{0sn}\|_2 + c_n)} > \left( \tilde{C} \sqrt{\tilde{q}_{0,sn}} + j \sqrt{n} \tau_n \right) \frac{1}{\sqrt{n_s}}$  for some absolute constant  $\tilde{C} > 0$  if  $\Theta_n \in \tilde{G}_{j,n}$ . Further applying Vershynin (2012, Equation 5.26), for all  $\Theta_n \in \tilde{G}_{j,n}$  we get

$$\mathbb{E}_{\Theta_n} (1 - \varphi_{sn}) \leq \Pr \left\{ \left\| \frac{1}{n_s} \sum_{i=1}^{n_s} \mathbf{z}_{s,i} \mathbf{z}_{s,i}^T - \mathbf{I}_{\tilde{q}_{0,sn}} \right\|_2 \geq \left( \tilde{C} \sqrt{\tilde{q}_{0,sn}} + j \sqrt{n} \tau_n \right) \frac{1}{\sqrt{n_s}} \right\} \leq e^{-K j^2 n_s \tau_n^2}.$$

Using (C1) we conclude  $\sup_{\Theta_n \in \tilde{G}_{j,n}} \mathbb{E}_{\Theta_n} (1 - \varphi_{sn}) \leq e^{-K' j^2 n \tau_n^2}$  for some  $K' > 0$ . □

## S.2.1 Technical Lemmas and Complete Proofs

**Proof of Lemma 2.** Lemma 2 closely resembles Theorem 8.22 from Ghosal and van der Vaart (2017). In the discussion following equation (8.22) in the book, the authors note that for the iid case, simpler theorems are obtained by using an absolute lower bound on the prior mass and by replacing the local entropy by the global entropy. In particular, (I)

implies Theorem 8.19(i) in the book. Similarly, (II) is the same condition in Theorem 8.20, and so the result follows.  $\square$

**Lemma 6.** *For any two matrices  $\mathbf{A}$  and  $\mathbf{B}$ ,*

- (i)  $s_{\min}(\mathbf{A}) \|\mathbf{B}\|_F \leq \|\mathbf{AB}\|_F \leq \|\mathbf{A}\|_2 \|\mathbf{B}\|_F$ .
- (ii)  $s_{\min}(\mathbf{A}) \|\mathbf{B}\|_2 \leq \|\mathbf{AB}\|_2 \leq \|\mathbf{A}\|_2 \|\mathbf{B}\|_2$ .
- (iii)  $s_{\min}(\mathbf{A}) s_{\min}(\mathbf{B}) \leq s_{\min}(\mathbf{AB}) \leq \|\mathbf{A}\|_2 s_{\min}(\mathbf{B})$ .

*Proof.* We borrow Lemma 6 from Pati *et al.* (2014) (Lemma 1.1. from the supplement).  $\square$

**Lemma 7.** *Let  $\mathbf{x} = (x_1, \dots, x_n)^T$  be a random vector with  $x_i \stackrel{\text{iid}}{\sim} N(0, \sigma^2)$  and  $\mathbf{x}_0 = (x_{01}, \dots, x_{0n})^T$  be a fixed vector. Then for some absolute constant  $C > 0$ ,  $\Pr(\|\mathbf{x} - \mathbf{x}_0\| \leq \tau) \geq e^{-C \max\{n \log \frac{\sqrt{\sigma}}{\tau}, n \log n, \frac{1}{\sigma^2} (\|\mathbf{x}_0\| + \tau)^2\}}$ .*

*Proof.* Let us first define  $v_n(r)$  to be the  $n$ -dimensional Euclidean ball of radius  $r$  centered at zero and  $|v_n(r)|$  denote its volume. For the sake of brevity, denote  $v_n = |v_n(1)|$ , so that  $|v_n(r)| = r^n v_n$ . Using Castillo and van der Vaart (2012, Lemma 5.3),  $v_n \asymp (2\pi e)^{n/2} n^{-(n+1)/2}$ .

Note that  $\Pr(\|\mathbf{x} - \mathbf{x}_0\| \leq \tau) \geq |v_n(\tau)| \inf_{\mathbf{z}: \|\mathbf{z} - \mathbf{x}_0\| \leq \tau} N_n(\mathbf{z}; \mathbf{0}, \sigma^2 \mathbf{I}_n)$  where  $N_n(\mathbf{z}; \boldsymbol{\mu}, \boldsymbol{\Sigma})$  denotes the density of a  $n$  dimensional multivariate normal distribution with mean  $\boldsymbol{\mu}$  and covariance matrix  $\boldsymbol{\Sigma}$  at the point  $\mathbf{z}$ . Now the greatest distance between the origin of the  $n$ -dimensional Euclidean space and the  $n$ -dimensional sphere of radius  $\tau$  centered at  $\mathbf{x}_0$  is bounded above by  $\|\mathbf{x}_0\| + \tau$ . Since the density of  $N_n(\mathbf{0}, \sigma^2 \mathbf{I}_n)$  at a point  $\mathbf{z}$  monotonically decreases with  $\|\mathbf{z}\|$ , we have  $\inf_{\mathbf{z}: \|\mathbf{z} - \mathbf{x}_0\| \leq \tau} N_n(\mathbf{z}; \mathbf{0}, \sigma^2 \mathbf{I}_n) \geq \frac{1}{(\sqrt{2\pi}\sigma)^n} e^{-\frac{1}{2\sigma^2} (\|\mathbf{x}_0\| + \tau)^2}$ . Hence for absolute constants  $C, C', C'' > 0$

$$\begin{aligned} \Pr(\|\mathbf{x} - \mathbf{x}_0\| \leq \tau) &\geq |v_n(\tau)| \inf_{\mathbf{z}: \|\mathbf{z} - \mathbf{x}_0\| \leq \tau} N_n(\mathbf{z}; \mathbf{0}, \sigma^2 \mathbf{I}_n) \\ &\geq C \tau^n (2\pi e)^{n/2} n^{-(n+1)/2} \times \frac{1}{(\sqrt{2\pi}\sigma)^n} e^{-\frac{1}{2\sigma^2} (\|\mathbf{x}_0\| + \tau)^2} \geq e^{n \log \frac{\tau}{\sqrt{\sigma}} - C' n (\log n + C'') - \frac{1}{2\sigma^2} (\|\mathbf{x}_0\| + \tau)^2} \end{aligned}$$

which concludes the proof.  $\square$

**Lemma 8.**

$$2\mathbb{KL}(\mathbb{P}_{0n} \parallel \mathbb{P}_n) = \sum_{s=1}^S n_s \left\{ \text{trace}(\boldsymbol{\Sigma}_{sn}^{-1} \boldsymbol{\Sigma}_{0sn} - \mathbf{I}_{dn}) - \log |\boldsymbol{\Sigma}_{sn}^{-1} \boldsymbol{\Sigma}_{0sn}| \right\} \leq \sum_{s=1}^S \frac{n_s \|\boldsymbol{\Sigma}_{sn} - \boldsymbol{\Sigma}_{0sn}\|_F^2}{\delta_{\min}^2 s_{\min}(\boldsymbol{\Sigma}_{sn})}.$$

*Proof.* Recall that  $\mathbb{P}_n$  and  $\mathbb{P}_{0n}$  denote the joint distributions of  $\mathcal{D}_n$  under  $\boldsymbol{\Theta}_n$  and the true value  $\boldsymbol{\Theta}_{0n}$ , respectively. Let  $f_{\mathbb{P}}(\mathbf{Y}_{s,i})$  denote the marginal distribution of  $\mathbf{Y}_{s,i}$  under a measure

$\mathbb{P}$ . Since  $f_{\mathbb{P}_n}(\mathbf{Y}_{s,i}) \equiv \text{N}_{d_n}(\mathbf{0}, \boldsymbol{\Sigma}_{sn})$  and  $f_{\mathbb{P}_{0n}}(\mathbf{Y}_{s,i}) \equiv \text{N}_{d_n}(\mathbf{0}, \boldsymbol{\Sigma}_{0sn})$  for all  $i$ , and the  $\mathbf{Y}_{s,i}$ s are independent, we have

$$\begin{aligned} \mathbb{KL}(\mathbb{P}_{0n} \parallel \mathbb{P}_n) &= \sum_{s=1}^S \sum_{i=1}^{n_s} \mathbb{KL}(f_{\mathbb{P}_{0n}}(\mathbf{Y}_{s,i}) \parallel f_{\mathbb{P}_n}(\mathbf{Y}_{s,i})) \\ &= \sum_{s=1}^S \frac{n_s}{2} \left\{ \text{trace}(\boldsymbol{\Sigma}_{sn}^{-1} \boldsymbol{\Sigma}_{0sn} - \mathbf{I}_{d_n}) - \log |\boldsymbol{\Sigma}_{sn}^{-1} \boldsymbol{\Sigma}_{0sn}| \right\}. \end{aligned} \quad (\text{S.20})$$

Let  $\mathbf{H} = \boldsymbol{\Sigma}_{sn}^{-\frac{1}{2}} \boldsymbol{\Sigma}_{0sn} \boldsymbol{\Sigma}_{sn}^{-\frac{1}{2}}$  and  $\mathbb{KL}_s = -\log |\boldsymbol{\Sigma}_{sn}^{-1} \boldsymbol{\Sigma}_{0sn}| + \text{trace}(\boldsymbol{\Sigma}_{0sn} \boldsymbol{\Sigma}_{sn}^{-1} - \mathbf{I}_{d_n})$ . Letting  $\psi_1, \dots, \psi_{d_n}$  be the eigenvalues of  $\mathbf{H}$ , we note that  $\mathbb{KL}_s = \sum_{j=1}^{d_n} \{(\psi_j - 1) - \log \psi_j\}$ . Observe that for any  $x > -1$ ,  $\log(1+x) \geq \frac{x}{1+x}$ ; additionally  $\psi_j > 0$  for all  $j = 1, \dots, d_n$  since these are eigenvalues of the positive definite matrix  $\mathbf{H}$ . Hence  $\log \psi_j \geq 1 - \frac{1}{\psi_j}$  implying that  $(\psi_j - 1) - \log \psi_j \leq \frac{(\psi_j - 1)^2}{\psi_j}$ . Therefore,

$$\mathbb{KL}_s \leq \sum_{j=1}^{d_n} \frac{(\psi_j - 1)^2}{\psi_j} = \|(\mathbf{H} - \mathbf{I}_{d_n})^2 \mathbf{H}^{-1}\|_F = \|(\boldsymbol{\Sigma}_{0sn} - \boldsymbol{\Sigma}_{sn})^2 \boldsymbol{\Sigma}_{sn}^{-1} \mathbf{H}^{-1} \boldsymbol{\Sigma}_{sn}^{-1}\|_F. \quad (\text{S.21})$$

Now  $\boldsymbol{\Sigma}_{sn} \mathbf{H} \boldsymbol{\Sigma}_{sn} = \boldsymbol{\Sigma}_{sn}^{\frac{1}{2}} \boldsymbol{\Sigma}_{0sn} \boldsymbol{\Sigma}_{sn}^{\frac{1}{2}}$ . Hence, from (S.21) and using Lemma 6 we arrive at

$$\mathbb{KL}_s \leq \|\boldsymbol{\Sigma}_{sn} - \boldsymbol{\Sigma}_{0sn}\|_F^2 \left\| (\boldsymbol{\Sigma}_{sn}^{\frac{1}{2}} \boldsymbol{\Sigma}_{0sn} \boldsymbol{\Sigma}_{sn}^{\frac{1}{2}})^{-1} \right\|_2 \leq \frac{\|\boldsymbol{\Sigma}_{sn} - \boldsymbol{\Sigma}_{0sn}\|_F^2}{s_{\min}(\boldsymbol{\Sigma}_{0sn}) s_{\min}(\boldsymbol{\Sigma}_{sn})} \leq \frac{\|\boldsymbol{\Sigma}_{sn} - \boldsymbol{\Sigma}_{0sn}\|_F^2}{\delta_{\min}^2 s_{\min}(\boldsymbol{\Sigma}_{sn})}.$$

Combining the above display with (S.20) we conclude the proof.  $\square$

**Lemma 9.** Assume that  $\|\boldsymbol{\Lambda}_n - \tilde{\boldsymbol{\Lambda}}_{0n}\|_F < \frac{C\tau_n}{q_{0n}\sqrt{c_n}}$ ,  $\max_s \|\mathbf{A}_{sn} - \tilde{\mathbf{A}}_{0sn}\|_F < \frac{C\tau_n}{c_n\sqrt{q_{0n}}}$ ,  $\|\boldsymbol{\Delta}_n - \boldsymbol{\Delta}_{0n}\|_F \leq C\tau_n$  and  $s_{\min}(\boldsymbol{\Delta}_n) > \nu$  where  $C = \nu\delta_{\min}^2/5$  and  $0 < \nu < \delta_{\min}^2$ . Then  $2\mathbb{KL}(\mathbb{P}_{0n} \parallel \mathbb{P}_n) \leq n\tau_n^2$ .

*Proof.* Using Lemma 8  $\mathbb{KL}(\mathbb{P}_{0n} \parallel \mathbb{P}_n) \leq \sum_{s=1}^S \frac{n_s \|\boldsymbol{\Sigma}_{sn} - \boldsymbol{\Sigma}_{0sn}\|_F^2}{2\delta_{\min}^2 s_{\min}(\boldsymbol{\Sigma}_{sn})}$ . Now  $\|\boldsymbol{\Sigma}_{sn} - \boldsymbol{\Sigma}_{0sn}\|_F \leq \|\boldsymbol{\Lambda}_n \boldsymbol{\Lambda}_n^T - \boldsymbol{\Lambda}_{0n} \boldsymbol{\Lambda}_{0n}^T\|_F + \|\boldsymbol{\Lambda}_{sn} \boldsymbol{\Lambda}_{sn}^T - \boldsymbol{\Lambda}_{0sn} \boldsymbol{\Lambda}_{0sn}^T\|_F + \|\boldsymbol{\Delta}_{0n} - \boldsymbol{\Delta}_n\|_F$  where  $\boldsymbol{\Lambda}_{sn} := \boldsymbol{\Lambda}_n \mathbf{A}_{sn}$  and  $\boldsymbol{\Lambda}_{0sn} := \boldsymbol{\Lambda}_{0n} \mathbf{A}_{0sn}$ . Recalling the notations defined in the beginning of Section S.2 we have

$$\begin{aligned} \|\boldsymbol{\Lambda}_{sn} \boldsymbol{\Lambda}_{sn}^T - \boldsymbol{\Lambda}_{0sn} \boldsymbol{\Lambda}_{0sn}^T\|_F &= \|\boldsymbol{\Lambda}_{sn} \boldsymbol{\Lambda}_{sn}^T - \tilde{\boldsymbol{\Lambda}}_{0sn} \tilde{\boldsymbol{\Lambda}}_{0sn}^T\|_F \\ &= \left\| (\boldsymbol{\Lambda}_{sn} - \tilde{\boldsymbol{\Lambda}}_{0sn}) \boldsymbol{\Lambda}_{sn}^T + \tilde{\boldsymbol{\Lambda}}_{0sn} (\boldsymbol{\Lambda}_{sn} - \tilde{\boldsymbol{\Lambda}}_{0sn})^T \right\|_F \\ &\leq \|\boldsymbol{\Lambda}_{sn} - \tilde{\boldsymbol{\Lambda}}_{0sn}\|_F \times \left( \|\boldsymbol{\Lambda}_{sn}\|_2 + \|\tilde{\boldsymbol{\Lambda}}_{0sn}\|_2 \right). \end{aligned} \quad (\text{S.22})$$

We define  $\Lambda_{sn} = \Lambda_n \mathbf{A}_{sn}$  and  $\tilde{\Lambda}_{0sn} = \tilde{\Lambda}_{0n} \tilde{\mathbf{A}}_{0sn}$ . Then using Lemma 6

$$\begin{aligned} \|\Lambda_{sn} - \tilde{\Lambda}_{0sn}\|_F &= \|\Lambda_n \mathbf{A}_{sn} - \tilde{\Lambda}_{0n} \tilde{\mathbf{A}}_{0sn}\|_F = \|\Lambda_n (\mathbf{A}_{sn} - \tilde{\mathbf{A}}_{0sn}) + (\Lambda_n - \tilde{\Lambda}_{0n}) \tilde{\mathbf{A}}_{0sn}\|_F \\ &\leq \|\Lambda_n\|_2 \|\mathbf{A}_{sn} - \tilde{\mathbf{A}}_{0sn}\|_F + \|\Lambda_n - \tilde{\Lambda}_{0n}\|_F \|\tilde{\mathbf{A}}_{0sn}\|_2. \end{aligned} \quad (\text{S.23})$$

Note that  $\|\Lambda_n - \tilde{\Lambda}_{0n}\|_F < \frac{C\tau_n}{q_{0n}\sqrt{c_n}} \Rightarrow \|\Lambda_n\|_2 \leq \|\Lambda_n\|_F \leq \|\tilde{\Lambda}_{0n}\|_F + \frac{C\tau_n}{q_{0n}\sqrt{c_n}} < \sqrt{c_n}$ . The last display holds since (C3)  $\Rightarrow \|\Lambda_{0n}\|_2 = o(\sqrt{c_n/q_{0n}}) \Rightarrow \|\Lambda_{0n}\|_F = o(\sqrt{c_n})$ . Combining the condition  $\max_{1 \leq s \leq S} \|\mathbf{A}_{sn} - \tilde{\mathbf{A}}_{0sn}\|_F \leq \frac{C\tau_n}{c_n\sqrt{q_{0n}}}$  and (S.23) we get

$$\max_{1 \leq s \leq S} \|\Lambda_{sn} - \tilde{\Lambda}_{0sn}\|_F \leq \sqrt{c_n} \times \frac{C\tau_n}{c_n\sqrt{q_{0n}}} + \frac{C\tau_n}{q_{0n}\sqrt{c_n}} \times \sqrt{q_{0n}} < \frac{2C\tau_n}{\sqrt{c_n q_{0n}}}. \quad (\text{S.24})$$

Now  $\|\Lambda_{sn} - \tilde{\Lambda}_{0sn}\|_F < \frac{C\tau_n}{\sqrt{c_n q_{0n}}} \Rightarrow \|\Lambda_{sn}\|_2 \leq \|\Lambda_{sn}\|_F < \|\tilde{\Lambda}_{0sn}\|_F + \frac{C\tau_n}{\sqrt{c_n q_{0n}}}$ . Note that  $\|\tilde{\Lambda}_{0sn}\|_F \leq \sqrt{q_{0sn}} \times \|\tilde{\Lambda}_{0sn}\|_2 \leq \sqrt{q_{0sn}} \times \|\Lambda_{0n}\|_2 \|\mathbf{A}_{0sn}\|_2 < \sqrt{c_n q_{0n}}$  implying that  $\|\Lambda_{sn}\|_2 + \|\tilde{\Lambda}_{0sn}\|_2 < 2\sqrt{c_n q_{0n}}$ . Combining the last display with (S.22) and (S.24) we obtain  $\|\Lambda_{sn} \Lambda_{sn}^T - \Lambda_{0sn} \Lambda_{0sn}^T\|_F \leq 2C\tau_n$ . Similarly  $\|\Lambda_n \Lambda_n^T - \Lambda_{0n} \Lambda_{0n}^T\|_F \leq \|\Lambda_n - \tilde{\Lambda}_{0n}\|_F (\|\Lambda_n\|_F + \|\tilde{\Lambda}_{0n}\|_F) \leq 2C\tau_n$ . Using the additional condition  $\|\Delta_n - \Delta_{0n}\|_F \leq C\tau_n$  and  $s_{\min}(\Delta_n) > \nu$ , we get  $\|\Sigma_{sn} - \Sigma_{0sn}\|_F \leq 5C\tau_n$ . Furthermore  $s_{\min}(\Sigma_{sn}) \geq s_{\min}(\Delta_n)$ . Hence,  $2\mathbb{KL}(\mathbb{P}_{0n} \parallel \mathbb{P}_n) \leq \sum_{s=1}^S \frac{n_s \|\Sigma_{sn} - \Sigma_{0sn}\|_F^2}{\delta_{\min}^2 s_{\min}(\Sigma_{sn})} \leq n\tau_n^2$ .  $\square$

**Lemma 10.** Recall the notations in Theorem 4. If  $\Theta_n \in G_{j,n}$ , then  $\frac{\|\Sigma_n - \Sigma_{0n}\|_2 - \epsilon_n c_n^2}{c_n^2 (\|\Sigma_n - \Sigma_{0n}\|_2 + c_n) (1 + \|\mathbf{A}_{sn}\|_2^2)} > \left( \tilde{C} \sqrt{\tilde{q}_{0,sn}} + j\sqrt{n}\tau_n \right) \frac{c_n^2}{\sqrt{n_s}}$  for some absolute constant  $\tilde{C} > 0$ .

*Proof.* For all  $\Theta_n \in \mathcal{P}_{1,n}$ ,  $1 + \|\mathbf{A}_{sn}\|_2^2 \leq Cn\tau_n^2$  for some  $C > 0$  for all  $s = 1, \dots, S$ . For brevity of notations, we define  $\omega = Cn\tau_n^2$ ,  $x = \|\Sigma_n - \Sigma_{0n}\|_2$  and  $a = \epsilon_n c_n^2$ . Hence observe that for  $\Theta_n \in G_{j,n}$

$$\begin{aligned} \frac{\|\Sigma_n - \Sigma_{0n}\|_2 - \epsilon_n c_n^2}{c_n^2 (\|\Sigma_n - \Sigma_{0n}\|_2 + c_n) (1 + \|\mathbf{A}_{sn}\|_2^2)} &> \left( \tilde{C} \sqrt{\tilde{q}_{0,sn}} + j\sqrt{n}\tau_n \right) \frac{1}{\sqrt{n_s}} \\ \Leftrightarrow \frac{x - a}{(x + c_n)\omega} &> \left( \tilde{C} \sqrt{\tilde{q}_{0,sn}} + j\sqrt{n}\tau_n \right) \frac{c_n^2}{\sqrt{n_s}} \Leftrightarrow x > \frac{a + \omega \left( \tilde{C} \sqrt{\tilde{q}_{0,sn}} + j\sqrt{n}\tau_n \right) \frac{c_n^3}{\sqrt{n_s}}}{1 - \omega \left( \tilde{C} \sqrt{\tilde{q}_{0,sn}} + j\sqrt{n}\tau_n \right) \frac{c_n^2}{\sqrt{n_s}}}. \end{aligned} \quad (\text{S.25})$$

The specifics on the postulated model from Section 3 imply  $\tilde{q}_{0,sn} \leq q_n + q_{sn} = o(n\tau_n^2)$ . As  $j = o\left[\frac{\sqrt{n}}{c_n^5} \{s_n q_{0n} \log(d_n q_n)\}^{-\frac{3}{2}}\right]$ ,  $\omega \left( \tilde{C} \sqrt{\tilde{q}_{0,sn}} + j\sqrt{n}\tau_n \right) \frac{c_n^2}{\sqrt{n_s}} \lesssim \frac{c_n^5}{\sqrt{n}} \{s_n q_{0n} \log(d_n q_n)\}^{\frac{3}{2}} = o(1)$

which can be seen from (D1). Therefore,  $\frac{a+\omega(\tilde{C}\sqrt{\tilde{q}_{0,sn}}+j\sqrt{n}\tau_n)\frac{c_n^3}{\sqrt{n_s}}}{1-\omega(\tilde{C}\sqrt{\tilde{q}_{0,sn}}+j\sqrt{n}\tau_n)\frac{c_n^2}{\sqrt{n_s}}}< a+j\times Cc_n^3\sqrt{\frac{(n\tau_n^2)^3}{n_s}}$  for some absolute constant  $C > 0$  and large enough  $n$ . Hence, (S.25) holds if  $x > a + j \times Cc_n^3\sqrt{\frac{(n\tau_n^2)^3}{n_s}}$  or equivalently if  $j\tau_n \leq e_n(\Theta_n, \Theta_{0n})$ , establishing the result.  $\square$

### S.3 Hamiltonian Monte Carlo Algorithm

Let  $\Pi(\Theta)$  be the target density where  $\Pi(\cdot)$  is differentiable with respect to  $\Theta \in \mathbb{R}^D$ . In HMC, a dynamical system is considered in which auxiliary “momentum” variables  $\mathbf{p} \in \mathbb{R}^D$  are introduced and the uncertain parameters  $\Theta$  in the target distribution are treated as the variables for the displacement. The total energy (Hamiltonian function) of the dynamical system is defined by  $H(\Theta, \mathbf{p}) = V(\Theta) + K(\mathbf{p})/2$ , where its potential energy  $V(\Theta) = -\log \Pi(\Theta)$  and its kinetic energy  $K(\mathbf{p}) = \mathbf{p}^T \mathbf{M}^{-1} \mathbf{p}$  depends only on  $\mathbf{p}$  and some chosen positive definite “mass” matrix  $\mathbf{M} \in \mathbb{R}^{D \times D}$ . The Hamiltonian dynamics will preserve the distribution  $e^{-H(\Theta, \mathbf{p})}$  and the invariant distribution will have  $\Pi(\cdot)$  to be the marginal distribution of  $\Theta$ . Using Hamilton’s equations, the evolution of  $\Theta, \mathbf{p}$  through “time”  $t$  is given by

$$\frac{d\mathbf{p}}{dt} = -\frac{\partial H}{\partial \Theta} = -\nabla V(\Theta), \quad \frac{d\Theta}{dt} = -\frac{\partial H}{\partial \mathbf{p}} = -\mathbf{M}^{-1} \mathbf{p}. \quad (\text{S.26})$$

If we start with  $\Theta(0)$  and draw a sample  $\mathbf{p}(0)$  from  $N(\mathbf{0}, \mathbf{M})$ , the final values  $\Theta(t), \mathbf{p}(t)$  will provide an independent sample  $\Theta(t)$  from  $\Pi$ . The leapfrog algorithm (Duane *et al.*, 1987) is popularly used to approximately solve the differential equations in (S.26). For time step  $\delta t$ , we have

$$\Theta(t + \delta t) = \Theta(t) + \delta t \mathbf{M}^{-1} \left[ \mathbf{p}(t) - \frac{\delta t}{2} \nabla V \{ \Theta(t) \} \right], \quad (\text{S.27})$$

$$\mathbf{p}(t + \delta t) = \mathbf{p}(t) - \frac{\delta t}{2} [\nabla V \{ \Theta(t) \} + \nabla V \{ \Theta(t + \delta t) \}]. \quad (\text{S.28})$$

The complete HMC sampler is summarized as follows for some  $\mathbf{M}$ ,  $\delta t$ , and  $L$  leapfrog steps. Thus we obtain the MCMC samples  $\Theta_1, \dots, \Theta_N$ .

---

#### Algorithm 3: Hamiltonian Monte Carlo

---

```

1 Initialize  $\Theta$  and simulate  $\mathbf{p}(0) \sim N(\mathbf{0}, \mathbf{M})$ .
2 for  $i = 1, \dots, N$  do
3   In iteration  $i$ , let the most recent sample be  $(\Theta_{i-1}, \mathbf{p}_{i-1})$ , then do the following to simulate a
      new sample  $(\Theta_i, \mathbf{p}_i)$ :
      (i) Randomly draw a new momentum vector  $\mathbf{p}'$  from  $N(\mathbf{0}, \mathbf{M})$ .
      (ii) Initiate the leapfrog algorithm with  $\{\Theta(0), \mathbf{p}(0)\} = (\Theta_{i-1}, \mathbf{p}')$  and run the algorithm (S.27)-(S.28)
           for  $L$  time steps to obtain a new candidate sample  $(\Theta'', \mathbf{p}'') = (\Theta(t + L\delta t), \mathbf{p}(t + L\delta t))$ .
      (iii) Set  $(\Theta_i, \mathbf{p}_i) = (\Theta'', \mathbf{p}'')$  with probability  $\min \left\{ 1, e^{H(\Theta'', \mathbf{p}'') - H(\Theta_{i-1}, \mathbf{p}')} \right\}$ .
4 end

```

---

## S.4 Extended Simulation Studies

### S.4.1 True Simulation Settings

#### Details on shared $\Lambda$ :

**Scenario 1:** We fill a consecutive 25% of the elements in each column of  $\Lambda$  with independent samples from  $\text{Unif}(-2, 2)$  and set the rest as zero. We choose the starting position of the consecutive non-zero elements randomly. To avoid having rows with all zero elements, we fill a randomly chosen 5 elements from each null row with iid samples from  $\text{Unif}(-2, 2)$ . A typical example for a  $200 \times 20$   $\Lambda$  is shown in the leftmost panel of Figure S.1.

**Scenario 2:** We separately fill the first and second consecutive  $d/2$  values in each column of  $\Lambda$ . For each half we follow the same strategy as scenario 1 and eliminate having entirely null rows using the aforementioned scheme. A typical example for a  $200 \times 20$   $\Lambda$  is shown in the middle panel of Figure S.1. From the correlation structures shown under the “True” panel of Figure 2 in the main paper, it can be seen that the above two scenarios induce very different correlation structures in the marginal distribution.

**Scenario 3:** We randomly choose and fill 25% of elements in each column of  $\Lambda$  with independent samples from  $\text{Unif}(-2, 2)$  and set the rest as zero. We eliminate null rows using the same strategy of scenario 1. A typical example for a  $200 \times 20$   $\Lambda$  is shown in the rightmost panel of Figure S.1.

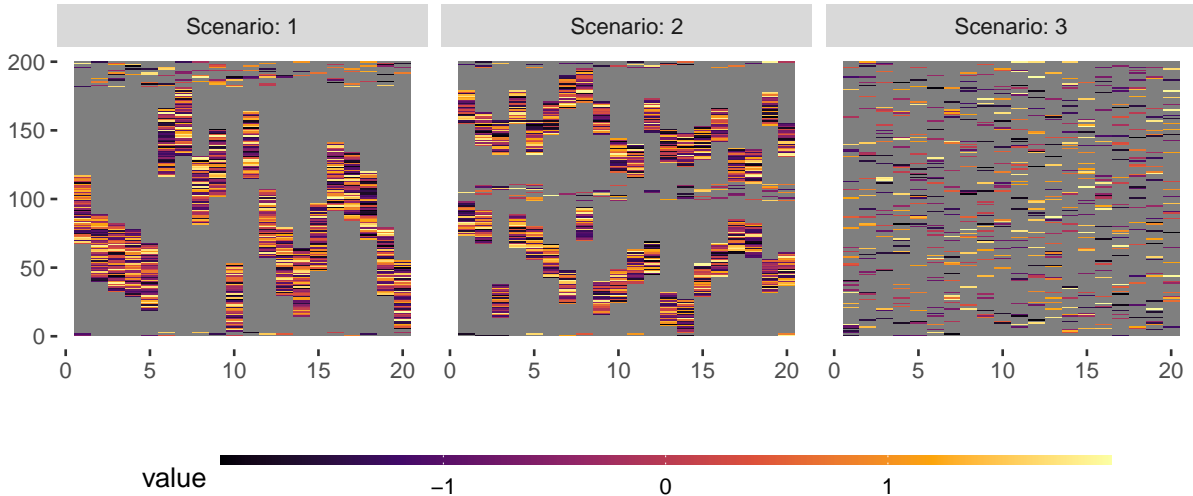


Figure S.1: Simulation truths of  $\Lambda$  across different scenarios under consideration. The gray color encodes exact 0 values.

#### Details on study-specific loadings:

**Slight misspecification:** We set the study-specific loading  $\Phi_s = \Lambda \mathbf{A}_s + \mathbf{E}_s$  where we generate  $\mathbf{A}_s = ((a_{s,j,h}))$  as  $a_{s,j,h} \stackrel{\text{iid}}{\sim} \mathcal{N}(0, 0.25^2)$  and  $\mathbf{E}_s = ((e_{s,j,h}))$  as  $e_{s,j,h} \stackrel{\text{iid}}{\sim} \mathcal{N}(0, 0.10^2)$ .

**Complete misspecification:** We generate the study-specific loading  $\Phi_s = ((\phi_{s,j,h}))$  as  $\phi_{s,j,h} \stackrel{\text{iid}}{\sim} N(0, 0.65^2)$ .

**Details on residual variance  $\Delta$ :** We set the diagonals of  $\Delta$  as 0.50.

### S.4.2 Recovering Shared Loading Matrix

In addition to the discussion in Section 5.1 in the main paper, here we include an extended simulation study showcasing recovery of the shared factor loading matrix  $\Lambda$ . We apply the post-processing strategy discussed in Section 2.1.2 on the MCMC samples to align them with respect to a common orthogonal rotation and then use the mean of the post-processed MCMC samples as a point estimate. The uncertainty quantification via the posterior samples guide inference on whether entries of  $\Lambda = ((\lambda_{j,h}))$  are 0 or not; following common practice in Bayesian inferences on sparsity patterns in matrices (Ksheera Sagar *et al.*, 2021), we set  $\lambda_{j,h} = 0$  if its 95% posterior credible interval includes 0.

**Comparison with alternate approaches:** Although the post-processing scheme aligns the MCMC samples of  $\Lambda$  with respect to a common orthogonal rotation, it is not immediately obvious whether the estimate  $\hat{\Lambda}$  is well-aligned with the simulation truth. To assess this, we further regress the columns of the true  $\Lambda$  on  $\hat{\Lambda}$ , and quantify accuracy in terms of the coefficient of determination  $R^2$ .

To this end, we regress  $\lambda_j$  on  $\hat{\Lambda}$  for all  $j = 1, \dots, q$ , where  $\lambda_j$  denotes the  $j^{th}$  column of the ground truth. Considering  $\hat{\Lambda}$  as the predictor matrix in this fashion, we expect  $R^2$  should

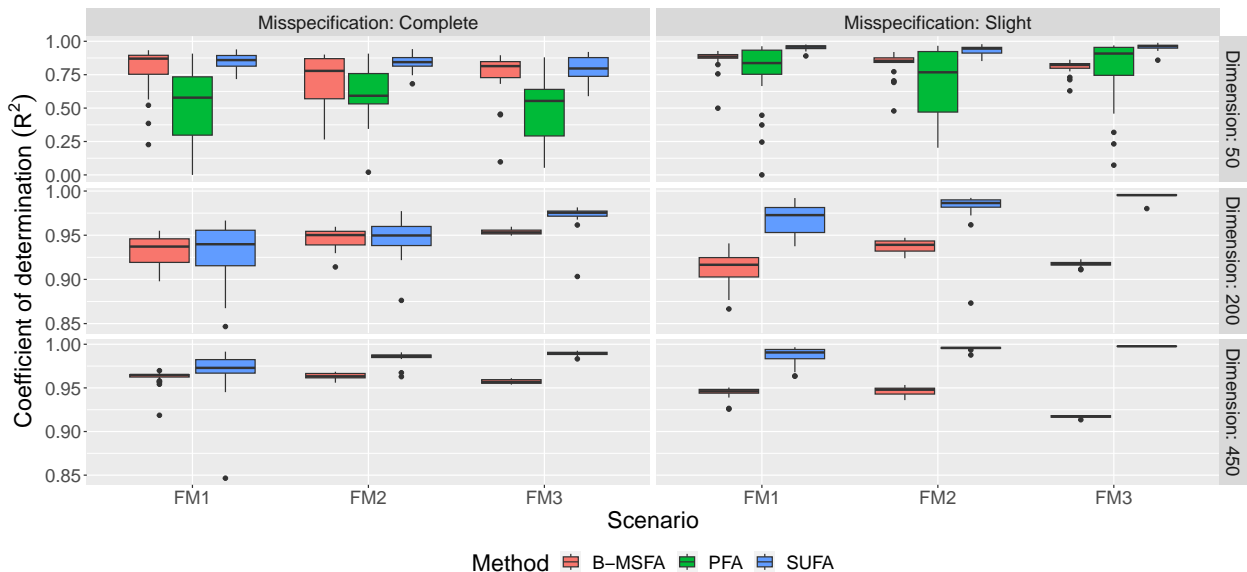


Figure S.2: Coefficient of determination  $R^2$  from regressing the columns of the true  $\Lambda$  on the estimated  $\hat{\Lambda}$  across all simulations settings and alternate approaches under consideration.

be close to 1 if the true  $\Lambda$  is well-learned up to orthogonal rotations, since the coefficient of determination is invariant under (non-singular) matrix multiplication. We report the median over the  $R^2$  values obtained from the  $q$  fitted regressions, and show the boxplots of the median  $R^2$  values from 25 independent replicates in Figure S.2, across all simulation settings together with estimates under peer methods. Note that the post-processing strategy in Section 2.1.2 does not depend on any prior specification or knowledge of  $\Lambda$ ; we use the same approach on samples from peer methods to obtain point estimates of  $\Lambda$ .

In Figure S.2, we see that even in the completely misspecified case, performance of our proposed SUFA is comparable with the other approaches, and evidently becomes better in higher dimensions. This is coherent with the observations reported in Section 5.1 in the main paper. The better performance of SUFA compared to B-MSFA is most likely due to nullification of the information switching issue allowing improved learning of the shared structure.

## S.5 Supplementary to Section 5.2

### S.5.1 Heatmaps of the Gene Expressions

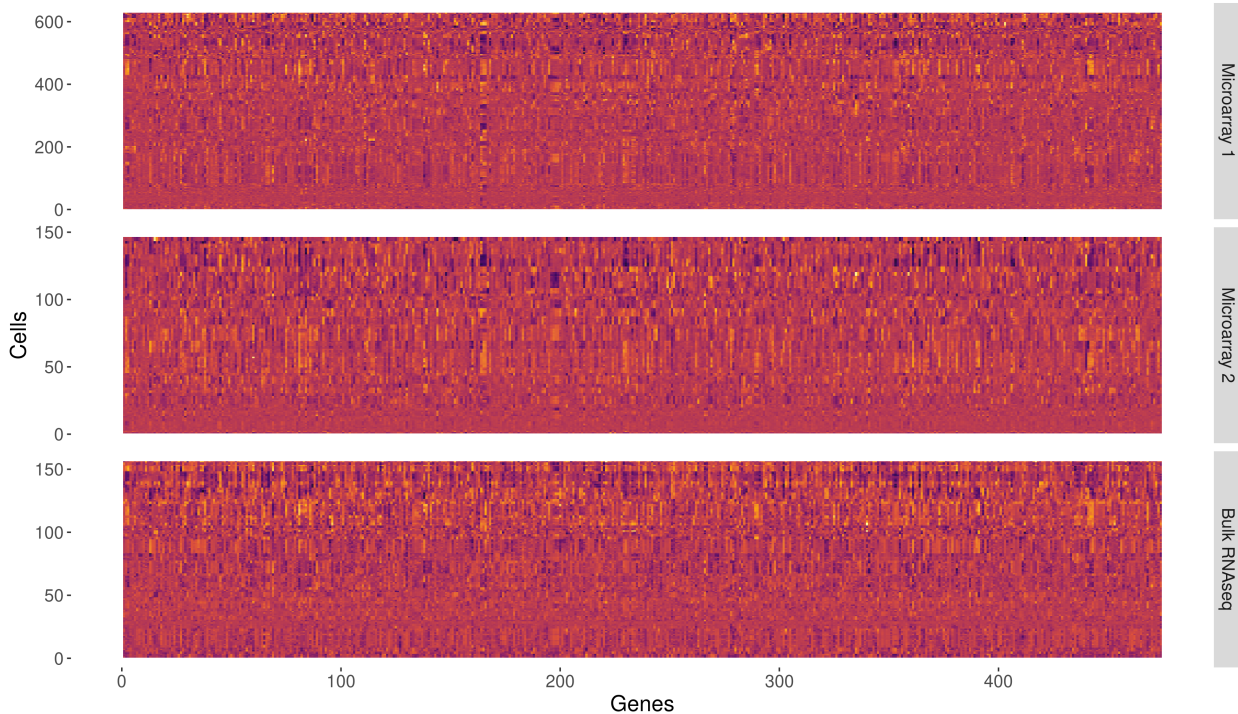


Figure S.3: Heatmaps of two microarray and a bulk RNAseq dataset on a common set of genes. The X and Y axes represent genes and cells across studies, respectively.

### S.5.2 Pre-processing the Data

The normalized dataset has more than 21,000 gene expressions from 628 and 146 immune cells in the two microarray datasets, respectively, and more than 49,000 genes from 156 cells in the bulk RNAseq dataset. We made a  $\log_2$  transformation of the data and filtered the top 5% genes with highest variances using the `genefilter` R package (Gentleman *et al.*, 2020) from each of the datasets and considered the intersection of the filtered genes in our analysis, resulting in a  $d = 474$  dimensional problem. Since different cell-types exhibit very different gene expression profiles, we centered the gene-expressions separately within each cell type.

## References

Banerjee, S. and Ghosal, S. (2015). Bayesian structure learning in graphical models. *Journal of Multivariate Analysis*, **136**, 147–162.

Bhattacharya, A., Pati, D., Pillai, N. S., and Dunson, D. B. (2015). Dirichlet-Laplace priors for optimal shrinkage. *Journal of the American Statistical Association*, **110**, 1479–1490.

Castillo, I. and van der Vaart, A. (2012). Needles and straw in a haystack: Posterior concentration for possibly sparse sequences. *The Annals of Statistics*, **40**, 2069–2101.

Duane, S., Kennedy, A., Pendleton, B. J., and Roweth, D. (1987). Hybrid Monte Carlo. *Physics Letters B*, **195**, 216–222.

Gentleman, R., Carey, V., Huber, W., and Hahne, F. (2020). *genefilter: methods for filtering genes from high-throughput experiments*. R package version 1.70.0.

Ghosal, S. and van der Vaart, A. (2017). *Fundamentals of nonparametric Bayesian inference*. Cambridge Series in Statistical and Probabilistic Mathematics. Cambridge University Press.

Ksheera Sagar, K. N., Banerjee, S., Datta, J., and Bhadra, A. (2021). Precision matrix estimation under the horseshoe-like prior-penalty dual. arXiv:2104.10750.

Pati, D., Bhattacharya, A., Pillai, N. S., and Dunson, D. (2014). Posterior contraction in sparse Bayesian factor models for massive covariance matrices. *The Annals of Statistics*, **42**, 1102–1130.

Vershynin, R. (2012). *Introduction to the non-asymptotic analysis of random matrices*, page 210–268. Cambridge University Press.